

ACEGEN: REINFORCEMENT LEARNING OF GENERATIVE CHEMICAL AGENTS FOR DRUG DISCOVERY

Albert Bou

Universitat Pompeu Fabra, Acellera

Morgan Thomas

Universitat Pompeu Fabra

Sebastian Dittert

Universitat Pompeu Fabra

Carles Navarro Ramírez

Acellera

Maciej Majewski

Acellera

Ye Wang

Biogen

Shivam Patel

PSIVANT

Gary Tresadern

Janssen Belgium

Mazen Ahmad

Janssen Belgium

Vincent Moens

PyTorch Team, Meta

Woody Sherman

PSIVANT

Simone Sciabola

Biogen

Gianni De Fabritiis

ICREA, Universitat Pompeu Fabra, Acellera

ABSTRACT

In recent years, reinforcement learning (RL) has emerged as a valuable tool in drug design, offering the potential to propose and optimize molecules with desired properties. However, striking a balance between capability, flexibility, and reliability remains challenging due to the complexity of advanced RL algorithms and the significant reliance on specialized code. In this work, we introduce ACEGEN, a comprehensive and streamlined toolkit tailored for generative drug design, built using TorchRL, a modern decision-making library that offers efficient and thoroughly tested reusable components. ACEGEN provides a robust, flexible, and efficient platform for molecular design. We validate its effectiveness by benchmarking it across various algorithms and conducting multiple drug discovery case studies. ACEGEN is accessible at <https://github.com/acellera/acegen-open>.

1 INTRODUCTION

Drug design is a complex process that involves the identification of biomolecules with multiple optimal properties, such as potency, selectivity, bioavailability, and toxicity. In recent years, a diversity of generative model solutions have been proposed as a promising approach to partially automate the process of proposing new molecules in the design-make-test-analysis cycle (Elton et al., 2019; Wang et al., 2022). These models typically employ machine learning algorithms to generate molecular candidates, but it remains challenging to efficiently search the vast chemical space to identify molecules with optimal properties (Brown et al., 2019), which is so large that it is not practically enumerable in a naive manner.

Reinforcement learning (RL) has emerged as a possible solution to explore this chemical space (Olivecrona et al., 2017; Popova et al., 2018) with an increasing focus on efficiency (Thomas et al., 2022; Guo et al., 2022). RL (Sutton & Barto, 2018) consists of a family of machine learning algorithms that use feedback as a learning signal. Through a trial and error process, RL algorithms can adapt their search strategy to the specific characteristics of compounds associated with desirable properties, and guide the generative models to propose novel molecules with similar characteristics. These methods use a customized reward function that assigns values to molecules, tailored specifically for the application or research question being addressed. To navigate the molecular space and find the most highly rewarded molecules, RL generative agents alternate between two phases: a data collection phase and a learning phase. During the data collection, molecules are generated by the generative model and scored based on the reward function. In the agent learning phase, the collected data is utilized to enhance the agent’s ability to generate interesting and relevant compounds. By

leveraging this feedback loop, the generative model can be continually improved to generate compounds with increasingly desirable properties. This is particularly interesting when the available chemical space cannot be enumerated and filtered using the scoring function, either because the scoring functions are very slow or because the search space is very large.

Currently, available implementations for drug discovery with RL rely heavily on custom code (Blaschke et al., 2020; Gao et al., 2022), favoring redundancy, complexity, limited efficiency and flexibility to incorporate a diverse set of solutions. However, the RL community already provides solutions to address these challenges. TorchRL, a comprehensive RL library (Bou et al., 2023), offers well-tested independent RL state-of-the-art components. In this work, we adopt TorchRL’s components as building blocks to assemble efficient and reliable drug discovery agents - a practice already successfully applied in diverse domains like drone control (Xu et al., 2024) and combinatorial optimization (Berto et al., 2023). This approach also fosters algorithmic research by enabling the encapsulation of new ideas within new components, which can seamlessly integrate with existing ones. TorchRL operates within the PyTorch ecosystem (Paszke et al., 2019), ensuring not only high-quality standards but also maintenance over time and future development.

To showcase the advantages of ACEGEN, we implement and evaluate well-known language-based algorithms for drug design. Language models can learn complex patterns in text and generate novel sequences, including molecular structures (Segler et al., 2018; Gómez-Bombarelli et al., 2018). Studies have focused on utilizing Simplified Molecular Input Line Entry System (SMILES) (Weininger, 1988), a string notation system used to represent chemical structures in a compact and standardized manner. Moreover, several prior studies have evidenced the benefits of combining generative language models and RL (Olivecrona et al., 2017; Fialková et al., 2021; Guo et al., 2022). Therefore, we re-implement three REINFORCE-based algorithms, REINFORCEWilliams (1992), REINVENT (Olivecrona et al., 2017) and AHC (Thomas et al., 2022). We also adapt general RL algorithms such as A2C (Mnih et al., 2016) and PPO (Schulman et al., 2017) to our problem setting. The REINVENT and the AHC methods use some level of experience replay, therefore we also add experience replay to REINFORCE. For this same reason, we also test PPOD (Libardi et al., 2021), a PPO-based algorithm adapted for experience replay.

To demonstrate the possible use cases and applications of ACEGEN, we have benchmarked these RL algorithms on a sample efficiency benchmark while considering chemistry, conducted an ablation study to better understand the components of a specific RL algorithm, tested a more challenging drug design relevant objective, and lastly presented RL for molecular constrained generative design.

ACEGEN code is accessible open source under the MIT license at <https://github.com/acellera/acegen-open> to facilitate uptake by the community.

2 METHODS

2.1 REINFORCEMENT LEARNING SETTING

Reinforcement learning tasks are formalized as Markov Decision Processes (MDPs) (Sutton & Barto, 2018). Formally, a MDP is described by a quintuple, denoted as $\langle S, A, R, P, \rho_0 \rangle$. Here, S represents the set of all possible states in the problem space, A denotes the set of valid actions available to the agent and $R : S \times A \times S \rightarrow \mathbb{R}$ defines the reward function, which assigns numerical values to transitions from one state to another based on the action taken. The function $P : S \times A \rightarrow \mathcal{P}(S)$ indicates the transition probability, with $P(s_{t+1}|s, a)$ representing the probability of transitioning to state s_{t+1} from the current state s under action a . Lastly, ρ_0 signifies the initial state distribution.

This approach naturally extends to the problem of sequentially designing molecules. In this context, a parameterized reinforcement learning (RL) policy, denoted as π_θ , guides molecule design by successively processing the current state representing a partially built molecule and selecting actions a_t to make changes to the molecule’s structure at each step until reaching a terminal state. The reward function evaluates the quality of the molecule, assigning a scalar value either at each generative step or at the end of the process when a complete compound is produced. Within this framework, $\pi_\theta(a_t|s_t)$ denotes the probability of the policy function parameterized by θ taking action a_t in state s_t . τ represents a complete sequence of actions needed to construct a molecule, often referred to

as an episode. $P(\tau|\theta)$ indicates the probability of a trajectory τ given the policy parameters θ . Furthermore, $R(\tau)$ represents the cumulative sum of rewards over the trajectory τ .

The goal of RL algorithms is to optimize the parameters of the policy π_θ to maximize $R(\tau)$. Different methods within the family of policy gradient methods (Sutton & Barto, 2018), such as REINFORCE (Williams, 1992), A2C (Advantage Actor-Critic) (Mnih et al., 2016), and PPO (Proximal Policy Optimization) (Schulman et al., 2017), are commonly used for this task. Additionally, various techniques can aid in training. Reward shaping involves modifying the reward function to provide additional feedback to the agent during training, potentially speeding up learning by providing more informative signals. Experience replay involves storing past experiences in a buffer and randomly sampling from it during training, which can improve sample efficiency and stabilize learning. Moreover, incorporating penalty terms, such as a Kullback-Leibler (KL) divergence loss term, can be utilized to encourage the agent to stay close to a reference or prior policy, helping to maintain stability and control the exploration-exploitation trade-off during training. Finally, ranking and selecting only the best K molecules in each given batch can improve efficiency. ACEGEN integrates all the aforementioned algorithms and additional techniques to form a comprehensive suite of state-of-the-art methods for molecular generation.

2.2 CHEMICAL LANGUAGE GENERATIVE MODELS

One possible approach to sequentially designing molecules is through string representations. Molecular string representations (Wiswesser, 1985) convert molecular graphs into strings and vice versa, allowing molecules to be encoded using specific syntactical rules. The task of molecular generation can then be formulated as a natural language processing (NLP) (Öztürk et al., 2020) problem. These have also been named Chemical Language Models (CLMs) (Grisoni, 2023). In this context, the resulting action space is discrete and each action is denoted also as a token. These actions are integrated by concatenating them to form a joint string representation, producing the next state. Each episode begins with a single special start token and can last for a varying number of steps. The episode ends when the agent chooses another special token called the stop token.

ACEGEN currently provides an environment for language model experimentation including SMILES (Weininger, 1988), DeepSMILES (O’Boyle & Dalke, 2018), SELFIES (Krenn et al., 2020), AtomInSmiles (Ucak et al., 2023) and SAFE (Noutahi et al., 2024) grammars, complemented by a user-friendly vocabulary class. Appendix A illustrates how the vocabulary and environment can be easily created and utilized for data generation.

In practice, CLMs are first trained unsupervised on a bulk of unlabeled data, aimed at learning to generate valid molecules, also referred to as pre-training, which is achieved through the application of the teacher enforcing method. (Lamb et al., 2016). The pre-trained CLM is the starting policy that can be further trained to optimize a specific objective with RL, similar to what happens in large language models. Moreover, this prior policy can be used as an anchor point from which the new RL policy should not deviate excessively.

ACEGEN currently provides pre-trained models for several architectures. More specifically, we provide GRU (Cho et al., 2014) policies pre-trained on two datasets: ChEMBL (Gaulton et al., 2012) and ZINC Gómez-Bombarelli et al. (2018). We also provide weights for an LSTM (Hochreiter & Schmidhuber, 1997) policy pre-trained on ChEMBL (Gaulton et al., 2012) and for a GPT2 (Radford et al., 2019) pre-trained on the REAL Database REAL lead-like compounds (Shivanyuk et al., 2007).

While our repository currently provides methods to create LSTM (Hochreiter & Schmidhuber, 1997), GRU (Cho et al., 2014), GPT2 Radford et al. (2019), Llama2 (Touvron et al., 2023) and Mamba (Gu & Dao, 2023) policies, practitioners can similarly include any other architectures of their choice taking advantage of current and future developments in NLP. Users can pre-train their policies with external code and integrate them without any need to modify the internal scripts of the library. Our repository contains a step-by-step tutorial that explains how to do the integration.

Finally, ACEGEN also provides its own pre-training script to train language models, either from ACEGEN or custom, to generate valid molecules through the teacher enforcing method (Lamb et al., 2016). Our code is engineered to adapt to the available computational resources, whether a single GPU or a distributed setup spanning multiple machines and GPUs. This adaptability allows us to efficiently train on datasets of large size.

2.3 SCORING AND EVALUATION OF MOLECULES

Scoring functions must reflect real-world drug design scenarios and be flexible enough to apply to a range of drug design challenges. Often, overly simplistic objective functions are used for optimization, such as penalized logP Jin et al. (2018), or complex solutions tailored to one particular generative model Blaschke et al. (2020).

ACEGEN allows the integration of custom scoring functions by providing the flexibility to define them as Python methods that accept strings and return numerical values. Alternatively, ACEGEN is optionally compatible with the MolScore Thomas et al. (2023) library, which offers a broad range of drug design relevant scoring functions, diversity filters, support for curriculum learning and also contains a benchmarking mode including MolOpt (Gao et al., 2022), GuacaMol (Brown et al., 2019), and others. Appendix B showcases how both scoring options can be accommodated within our codebase. Additionally, the library offers a detailed tutorial, guiding users through the process of implementing and incorporating custom scoring functions seamlessly into the entire workflow to train agents with them.

2.4 RL AGENTS TRAINING

ACEGEN provides training for RL agents utilizing the methods: REINFORCE (Williams, 1992), REINVENT Blaschke et al. (2020), AHC Thomas et al. (2022), A2C Mnih et al. (2016) and PPO Schulman et al. (2017) and an adaptation of the PPO Libardi et al. (2021) algorithm. We deviate from the exact implementation of PPO by omitting the use of an initial expert demonstration, refraining from replaying episodes with high-value predictions (only episodes with high rewards are replayed) and employing a fixed amount of replay data per batch. All methods are fully configurable to allow the use of custom scoring functions and models beyond those already provided by the library.

REINVENT and AHC can be considered extensions of the REINFORCE algorithm. More specifically, REINVENT incorporates reward shaping, experience replay, and a penalty for high-likelihood sequences into the basic REINFORCE framework. Additionally, AHC ranks and selects the top K molecules in each batch of data. We find the reward shaping not to be compatible with advantage-based methods and the high-likelihood penalty term detrimental, therefore for A2C, PPO and PPOD we introduce instead a term to the loss function based on the Kullback-Leibler divergence (KL) between the actor policy and a prior policy. This term serves to penalize the policy for deviating too much from a prior, similar in concept to reward shaping in REINVENT and AHC. The incorporation of KL constraints is a common practice in research papers aligning language models with custom reward functions, as seen in examples utilizing human feedback Menick et al. (2022); Ouyang et al. (2022); Bai et al. (2022).

2.5 DE-NOVO, DECORATIVE AND FRAGMENT-LINKING GENERATION

In drug discovery pipelines, generating molecules from scratch may not always suffice. To meet diverse requirements, ACEGEN offers multiple sampling modes. PromptSMILES (Thomas et al., 2024) is a simple method enabling constrained molecule generation using models pre-trained solely with teacher enforcement on full SMILES, making it possible to generate molecules while adhering to specific chemical sub-structures. Specifically, in addition to de-novo generation, ACEGEN scripts allow for easy configuration of scaffold decoration and fragment-linking molecule generation modes. Constrained sampling modifies only the data collection behavior, operating independently of all other agent components, in line with the TorchRL philosophy. Tutorials on performing constrained generation are provided within the repository.

3 RESULTS

To showcase some of the use cases of ACEGEN, we have benchmarked multiple methods in chemistry benchmarks, conducted an ablation study on REINVENT, tested a challenging drug design objective, and explored constrained RL with PromptSMILES.

3.1 BENCHMARKING RL PERFORMANCE

To assess different RL algorithms, we have compared performance on the Practical Molecular Optimization (MolOpt) benchmark Gao et al. (2022) as implemented in MolScore (Thomas et al., 2023). This benchmark encompasses 23 distinct tasks associated with different objectives to be optimized within a budget of 10,000 molecules. All algorithms use the same GRU policy model architecture as in the original MolOpt benchmark, implemented in ACEGEN and pretrained on a curated subset of ChEMBL (Gaulton et al., 2012). We compared REINFORCE (Williams, 1992), REINVENT with the hyperparameters from the original paper (Blaschke et al., 2020), REINVENT-MolOpt with optimized hyperparameters for the MolOpt benchmark (Gao et al., 2022), and AHC with the hyperparameters from the original paper (Thomas et al., 2022). Note that we utilize experience replay in all of the aforementioned algorithms. Then we also test A2C (Mnih et al., 2016), PPO (Schulman et al., 2017) which does not utilize any experience replay, and PPOD (Libardi et al., 2021) which is an adaptation of PPO to accommodate experience replay. All algorithms are ACEGEN implementations, and the hyperparameter values used for all of them are provided in our repository. As a sanity check, we compared our implementation of REINVENT with the implementation used in the MolOpt paper. Our simplified re-implementation achieved better results with faster training. These results are shown in Appendix C.

As proposed by the MolOpt benchmark authors, Table 1 shows algorithm performance on the AUC of the top 10 molecules as an indication of the sample efficiency of identifying 10 desirable molecules with respect to the objective, a representative figure that might be carried forward to later stages of drug design. This shows that PPOD is state-of-the-art with respect to sample efficiency, followed by REINVENT-MolOpt and then PPO. To achieve a higher level understanding of performance, Table 2 shows a selection of metrics aimed to measure maximum performance, efficiency, and exploration (a common trade-off with exploitation and hence efficiency in RL). These results show that REINVENT-MolOpt achieves maximum performance as measured by the average top 10 molecules, PPOD maximum efficiency as measured by AUC of the top 10 molecules, and AHC maximum exploration as measured by the number of unique compounds generated.

Task	ACEGEN REINFORCE	ACEGEN REINVENT	ACEGEN REINVENT-MolOpt	ACEGEN AHC	ACEGEN A2C	ACEGEN PPO	ACEGEN PPOD
Albuterol_similarity	0.68 ± 0.03	0.69 ± 0.02	0.90 ± 0.01	0.77 ± 0.02	0.82 ± 0.04	0.93 ± 0.02	0.94 ± 0.00
Amlodipine_MPO	0.55 ± 0.01	0.56 ± 0.01	0.65 ± 0.06	0.56 ± 0.01	0.55 ± 0.01	0.58 ± 0.03	0.68 ± 0.02
C7H8N2O2	0.83 ± 0.01	0.82 ± 0.03	0.90 ± 0.02	0.76 ± 0.04	0.84 ± 0.04	0.89 ± 0.01	0.89 ± 0.03
C9H10N2O2PF2Cl	0.70 ± 0.02	0.70 ± 0.02	0.76 ± 0.03	0.68 ± 0.02	0.69 ± 0.03	0.66 ± 0.02	0.79 ± 0.02
Celecoxib_rediscovery	0.63 ± 0.02	0.64 ± 0.03	0.77 ± 0.02	0.72 ± 0.02	0.73 ± 0.06	0.65 ± 0.12	0.82 ± 0.03
DRD2	0.98 ± 0.00	0.97 ± 0.00	0.99 ± 0.00	0.98 ± 0.01	0.98 ± 0.01	0.99 ± 0.00	0.99 ± 0.00
Deco_hop	0.63 ± 0.00	0.63 ± 0.01	0.67 ± 0.01	0.64 ± 0.01	0.62 ± 0.00	0.62 ± 0.01	0.66 ± 0.02
Fexofenadine_MPO	0.71 ± 0.01	0.71 ± 0.00	0.80 ± 0.03	0.72 ± 0.00	0.71 ± 0.00	0.73 ± 0.00	0.78 ± 0.01
GSK3B	0.84 ± 0.01	0.84 ± 0.02	0.92 ± 0.02	0.82 ± 0.01	0.85 ± 0.02	0.90 ± 0.02	0.92 ± 0.02
JNK3	0.75 ± 0.03	0.75 ± 0.02	0.85 ± 0.04	0.75 ± 0.01	0.74 ± 0.06	0.80 ± 0.04	0.87 ± 0.02
Median_molecules_1	0.26 ± 0.00	0.24 ± 0.00	0.36 ± 0.02	0.24 ± 0.00	0.31 ± 0.01	0.33 ± 0.02	0.35 ± 0.02
Median_molecules_2	0.22 ± 0.00	0.22 ± 0.00	0.28 ± 0.01	0.24 ± 0.00	0.25 ± 0.01	0.25 ± 0.02	0.29 ± 0.01
Mestranol_similarity	0.60 ± 0.03	0.55 ± 0.04	0.85 ± 0.07	0.66 ± 0.04	0.69 ± 0.07	0.75 ± 0.15	0.89 ± 0.05
Osimertinib_MPO	0.82 ± 0.01	0.82 ± 0.00	0.86 ± 0.01	0.83 ± 0.00	0.81 ± 0.01	0.82 ± 0.01	0.84 ± 0.00
Perindopril_MPO	0.48 ± 0.01	0.47 ± 0.00	0.54 ± 0.01	0.47 ± 0.01	0.48 ± 0.00	0.50 ± 0.01	0.53 ± 0.00
QED	0.94 ± 0.00	0.94 ± 0.00	0.94 ± 0.00	0.94 ± 0.00	0.94 ± 0.00	0.94 ± 0.00	0.94 ± 0.00
Ranolazine_MPO	0.70 ± 0.01	0.69 ± 0.00	0.76 ± 0.01	0.70 ± 0.00	0.74 ± 0.01	0.73 ± 0.01	0.75 ± 0.00
Scaffold_hop	0.80 ± 0.00	0.79 ± 0.00	0.86 ± 0.02	0.80 ± 0.01	0.80 ± 0.00	0.80 ± 0.02	0.84 ± 0.03
Sitagliptin_MPO	0.34 ± 0.02	0.33 ± 0.01	0.38 ± 0.03	0.33 ± 0.02	0.39 ± 0.02	0.32 ± 0.02	0.39 ± 0.02
Thiothixene_rediscovery	0.41 ± 0.01	0.41 ± 0.00	0.56 ± 0.04	0.45 ± 0.02	0.48 ± 0.04	0.48 ± 0.06	0.58 ± 0.09
Troglitazone_rediscovery	0.31 ± 0.02	0.31 ± 0.02	0.47 ± 0.05	0.34 ± 0.01	0.35 ± 0.02	0.46 ± 0.07	0.52 ± 0.06
Valsartan_smarts	0.03 ± 0.00	0.02 ± 0.00	0.02 ± 0.00	0.02 ± 0.00	0.02 ± 0.00	0.03 ± 0.00	0.03 ± 0.00
Zaleplon_MPO	0.47 ± 0.01	0.47 ± 0.01	0.52 ± 0.01	0.48 ± 0.01	0.47 ± 0.01	0.50 ± 0.02	0.52 ± 0.01
Total	13.67	13.60	15.65	13.91	14.27	14.65	15.80

Table 1: Algorithm comparison for the Area Under the Curve (AUC) of the top 10 molecules on MolOpt benchmark objectives. This metric captures the sample efficiency in identifying 10 desirable molecules with respect to the objective. Each algorithm was run 5 times with different seeds, and results were averaged.

3.2 BENCHMARKING RL PERFORMANCE FOR PRACTICAL DRUG DISCOVERY

RL optimizes the policy for the cumulative future rewards as provided by either one or a sum of multiple scoring functions. However, in practical drug discovery, it is not straightforward to write the precise scoring functions that are needed and how to weigh them into a single scalar. For exam-

Metric	ACEGEN REINFORCE	ACEGEN REINVENT	ACEGEN REINVENT-MolOpt	ACEGEN AHC	ACEGEN A2C	ACEGEN PPO	ACEGEN PPOD
Valid	21.77	21.78	21.74	21.45	18.93	21.78	21.52
Top-10 Avg	15.85	15.69	17.43	16.09	15.67	15.63	17.10
Top-10 AUC	13.67	13.60	15.65	13.91	14.27	14.65	15.80
Unique	22.28	22.63	13.68	22.68	18.38	9.47	10.21
B&T-CF	14.34	14.74	7.00	13.77	7.82	5.81	5.71
B&T-CF Top-10 Avg (Div)	14.83	14.79	16.06	15.25	14.54	14.60	15.78
B&T-CF Top-10 AUC (Div)	12.85	12.81	14.61	13.11	13.32	13.67	14.60
B&T-CF Diversity (SEDiv@1k)	17.39	18.19	10.10	17.55	14.24	8.47	7.96

Table 2: Algorithm comparison on a selection of metrics analyzing the performance on the MolOpt benchmark. Valid is a sanity check that measures the proportion of valid molecules generated. Top-10 AUC is a measure of sample efficiency as shown in 1. Top-10 Avg is a measure of the absolute best 10 molecules achieved with the budget. Unique is a proxy for exploration which measures the proportion of unique molecules generated. Basic and target chemistry filters (B&T-CF) are the proportion of molecules after filtering out highly idiosyncratic molecules in general or with respect to the pretraining dataset. The B&T-CF Top-10 AUC and B&T-CF Top-10 Avg are recalculated on this subset while also enforcing that the 10 molecules identified offer diverse solutions (Div). Lastly, B&T-CF Diversity is a proxy measure of exploration via sphere exclusion diversity Thomas et al. (2021) on this subset. Each algorithm was run 5 times with different seeds, and results were averaged and then summed over the 23 tasks. A perfect score for all metrics is 23.

ple, scoring functions can sometimes not produce the desired chemistry, or show clear exploitation loopholes Renz et al. (2019); Langevin et al. (2022). In this setting, a sufficient element of regularization to a prior policy is useful, as the prior policy has learned a chemical space distribution based on a specified training dataset of choice which acts as a representation of desirable chemistry by examples. It is for this reason that methods like REINVENT have been designed heuristically to contain terms that try to enforce regularization instead of entirely using the reward signal.

To account for this, we make a modification to the average and AUC of the top 10 molecules to ensure they are diverse by an ECFP4 Tanimoto similarity of less than 0.35 to each other. Moreover, we use sphere exclusion diversity (SEDiv@1k) of de novo molecules Thomas et al. (2021) which measures the proportion of molecules needed to describe chemical space in a random sample of 1,000 molecules, as a proxy for exploration. This is more representative than the number of unique molecules that could all reside in a close area of chemical space. Lastly, we remove de novo molecules that do not pass a series of filters. This includes a basic chemistry filter (B-CF): logP less than or equal to 4.5, rotatable bond count less than or equal to 7, molecular weight in the range 150 to 650 Da, only contain atoms belonging to the following set $A \in \{C, S, O, N, H, F, Cl, Br\}$, and do not violate the substructure alerts as described in Polykovskiy et al. (2020). Moreover on the assumption that the training dataset describes desirable chemistry by examples, a target chemistry filter (T-CF): logP and molecular weight within $\mu \pm 4\sigma$ of the training dataset distribution, as well as, removing any molecule that comprises $> 10\%$ novel atomic environment bits with respect to the reference molecules, as measured by ECFP4 bits (an example of this is shown in Figure 8). The combination of the basic and target chemistry filter is denoted (B&T-CF).

Re-evaluating RL performance with these new metrics (Table 2) it can be seen that a smaller proportion of molecules pass the chemistry filters for REINVENT-MolOpt, A2C, PPO, and PPOD, as expected due to decreased regularization terms to optimize efficiency. Despite this, REINVENT-MolOpt achieves the highest score for the average and AUC of the top 10 diverse molecules followed by PPOD. As a proxy for exploration, REINVENT contains the highest sphere exclusion diversity followed by AHC. Interestingly, REINFORCE maintains a high proportion of molecules passing the chemistry filters despite no explicit regularization term, outperforming REINVENT in absolute performance and efficiency. Table 3 shows the alternative approach of explicitly including these requirements in the reward signal by the addition of the chemistry filters and a diversity filter to each objective. As expected, including these requirements explicitly in the reward function increases the proportion of molecules passing these filters. However, every algorithm drops in performance as measured by the average and AUC top 10 diverse molecules that pass the filters. In this case showing that better overall score optimization and efficiency (including those that measure the quality of chemistry) is achieved by implicit regularization to the prior policy. This could be a result of the specific implementation of the chemistry filters in the reward resulting in a score of 0 if they do not pass; however, optimal implementation of reward signal can in itself be considered an art. There-

fore, simpler reward signals are usually better, and, achieving desirable chemistry by regularization enables the design of a simpler reward signal. The fine-tuning of the optimization algorithm, reward signals and regularization might be target-dependent and goes beyond the scope of this work, but it is enabled by ACEGEN.

Metric	MolOpt					MolOpt-CF				
	ACEGEN REINFORCE	ACEGEN REINVENT	ACEGEN REINVENT-MolOpt	ACEGEN AHC	ACEGEN PPOD	ACEGEN REINFORCE	ACEGEN REINVENT	ACEGEN REINVENT-MolOpt	ACEGEN AHC	ACEGEN PPOD
Valid	21.77	21.79	21.74	21.45	21.52	22.00	21.95	21.65	21.71	21.05
Top-10 Avg	15.85	15.67	17.43	16.09	17.10	14.76	14.54	16.17	14.86	15.18
Top-10 AUC	13.67	13.55	15.65	13.91	15.80	12.94	12.78	14.57	13.00	14.01
Unique	22.28	22.67	13.68	22.68	10.21	22.44	22.83	16.63	22.80	14.13
B&T-CF	14.34	14.70	7.00	13.77	5.71	18.44	18.59	13.62	17.72	11.55
B&T-CF Top-10 Avg (Div)	14.95	14.79	16.06	15.25	15.78	14.51	14.33	15.92	14.68	14.86
B&T-CF Top-10 AUC (Div)	12.91	12.81	14.61	13.11	14.60	12.79	12.66	14.35	12.89	13.74
B&T-CF Diversity (SEDiv@1k)	17.39	18.23	10.10	17.55	7.96	16.23	17.65	7.97	17.33	7.92

Table 3: Comparison of algorithm performance with or without explicit chemistry filters included in the reward signal as a scoring function. MolOpt is the normal benchmark and MolOpt-CF is the benchmark with chemistry filters and a diversity filter applied to each objective.

3.3 ABLATION STUDY OF THE REINVENT ALGORITHM

One of the most common RL algorithms used for the fine-tuning of CLMs is REINVENT Olivecrona et al. (2017). From a theoretical RL perspective, this algorithm can be viewed as a reward shaping of the REINFORCE algorithm. However, the derivation of this specific reward-shaping mechanism is unclear. Therefore, using the modular components of ACEGEN we have conducted an ablation study to better understand the impact of the reward shaping, experience replay and sequence likelihood penalty that together comprise the components of the REINVENT algorithm. For this comparison, we used the default recommended REINVENT hyperparameters and measured performance on the MolOpt benchmark. With respect to maximum performance and efficiency, Table 4 shows that the primary performance improvement comes from the addition of experience replay to REINFORCE. While the addition of the reward shaping mechanism does improve over REINFORCE, the combination of experience replay and reward shaping does not improve over REINFORCE with experience replay. However, the addition of reward shaping that couples the agent policy to the prior policy does lead to an improved quality of chemistry as measured by the proportion of valid and unique molecules that also pass the chemistry filters, but at the compromise of performance. The results further emphasize the utility of adding regularisation in practical applications, as discussed in the previous section. In the original implementation, the authors of REINVENT also include a loss term to penalize highly likely sequences. Table 4 shows that this primarily increases exploration but to the detriment of all other metrics, including decreasing the proportion of molecules that pass chemistry filters, moreover, if used without reward shaping it leads to a complete collapse in learning.

Metric	REINFORCE	REINFORCE	REINFORCE	REINFORCE	REINFORCE	REINFORCE ¹
	-	+ replay	-	+ replay	-	+ replay
Valid	21.74	21.77	21.93	21.90	21.76	21.78
Top-10 Avg	14.74	15.85	14.80	15.69	14.79	15.69
Top-10 AUC	13.21	13.67	13.21	13.57	13.11	13.60
Unique	22.35	22.28	22.46	22.29	22.80	22.63
B&T-CF	14.15	14.34	15.31	15.08	14.83	14.74
B&T-CF Top-10 Avg (Div)	13.81	14.95	13.88	14.80	13.89	14.83
B&T-CF Top-10 AUC (Div)	12.51	12.91	12.48	12.83	12.38	12.85
B&T-CF Diversity (SEDiv@1k)	17.61	17.39	17.93	17.52	18.76	18.19

Table 4: Ablation study of REINFORCE algorithm on the MolOpt benchmark with and without separate components including experience replay, reward shaping, and a high sequence likelihood penalty. Each algorithm was run 5 times with different seeds, and results were averaged and then summed over the 23 tasks. Note that all components together constitute the ACEGEN REINVENT implementation with default hyperparameters.

3.4 CASE STUDY: DE-NOVO GENERATION IN THE 5-HT_{2A}

To reflect more realistic situations that may arise in practical drug discovery scenarios, we apply the different RL algorithms implemented on a more challenging objective previously proposed by

Thomas et al. (2023). This objective is designing 5-HT_{2A} receptor ligands selective over the highly related D₂ receptor utilizing only structural information. This is an important and relevant challenge as clinically, this off-target profile leads to undesirable extrapyramidal side-effects in the treatment of psychosis Casey et al. (2022). To achieve this, this objective aims to minimize the docking score against 5-HT_{2A} (PDB: 6A93), yet maximize the docking score against D₂ (PDB: 6CM4), within a budget of 32,000 molecules. Both crystal structures are co-crystallized with Risperidone, reflecting the high degree of binding pocket similarity. In contrast to the proposed objective configuration, we use rDock Ruiz-Carmona et al. (2014) due to more permissive licensing.

Metric	ACEGEN REINFORCE	ACEGEN REINVENT	ACEGEN REINVENT-MolOpt	ACEGEN AHC	ACEGEN A2C	ACEGEN PPO	ACEGEN PPOD
Valid	0.95	0.96	0.93	0.94	0.98	0.94	0.95
Top-10 Avg	1.05	1.09	1.10	1.10	1.04	1.06	1.07
Top-10 AUC	1.02	1.05	1.05	1.05	1.02	1.01	1.02
Unique	1.00	1.00	0.89	1.00	1.00	0.99	0.99
B&T-CF	0.71	0.71	0.45	0.63	0.27	0.59	0.48
B&T-CF Top-10 Avg (Div)	1.05	1.06	1.08	1.10	1.02	1.02	1.03
B&T-CF Top-10 AUC (Div)	1.01	1.03	1.04	1.05	1.00	0.99	0.99
B&T-CF Diversity (SEDiv@1k)	0.89	0.91	0.64	0.89	0.77	0.60	0.53

Table 5: Performance summary of algorithms on 5-HT_{2A} case study. Including after applying a basic chemistry filter (B-CF) as described previously. B-CF is the fraction of molecules that pass the chemistry filter. Note that the values here are re-normalized based on the scores achieved for a subset of 5-HT_{2A} ligands that display at least 2-fold selectivity over D₂ as extracted from ChEMBL31 Gaulton et al. (2012). Therefore, a score of 0.91 indicates the best score observed in the known ligand subset, and a score greater than 1.0 indicates that a single molecule achieves both a better (more negative) 5-HT_{2A} docking score and (more positive) D₂ docking score than seen anywhere in the known subset.

A summary of performance can be shown in the metrics in Table 5. These results show that when considering both optimization performance and chemistry - which is not explicitly captured in the objective - AHC achieves the highest average top 10 molecules and sample efficiency while maintaining high rates of molecules that pass chemistry filters and high diversity. This objective greater highlights the utility of compromising performance for regularization in practice, compared to the MolOpt benchmark which favours exploitation. A demonstration of de novo molecules and their predicted docked pose in 5-HT_{2A} is shown in Figure 1, for further methods, analysis and interpretation of the differences between RL algorithms from a chemistry perspective see Appendix E.

3.5 CASE STUDY: SCAFFOLD CONSTRAINED GENERATION

ACEGEN can conduct constrained generation by leveraging PromptSMILES Thomas et al. (2024) which proposes iterative CLM prompting on SMILES in combination with RL to achieve fine-tune a pre-trained CLMs to the task of constrained generation. Here we demonstrate this application with two experiments: 1) scaffold decoration via known synthetic reactions as proposed with LibINVENT Fialková et al. (2021), and 2) scaffold decoration followed by scaffold-constrained docking to explore growth vectors inside a binding pocket.

In the first experiment, we compared the performance of RL algorithms on two tasks proposed with LibINVENT Fialková et al. (2021), both of which conduct scaffold decoration of a piperazine core with an amine linker moiety commonly present in D₂ receptor ligands. As in the MolOpt benchmark, we apply a budget of 10,000 molecules. The first task is to optimize the predicted probability of D₂ activity as evaluated by a QSAR model. The second task adds a selective reaction filter, rewarding piperazine growth via a Buchwald reaction and amine linker growth via an amide coupling reaction. Table 6 shows successful optimization of both objectives, with AHC performing best on the first task, and REINVENT (either with default or MolOpt parameters) performing best on the second task. However, all algorithms except A2C are able to solve the task with a yield above 90%, and fully satisfy the selective reaction objectives in 80 to 90% of molecules.

In the second experiment, we used PromptSMILES in combination with AHC (based on the superior performance in the 5-HT_{2A} case study) to conduct scaffold decoration in the catalytic site of BACE1, a key therapeutic target for the treatment of Alzheimer’s disease. Here we used the reference structure 4B05 co-crystallized with AZD3839 Jeppsson et al. (2012) which is a typical BACE1 inhibitor consisting of an amidine core interacting with two catalytic aspartates, and occupation of

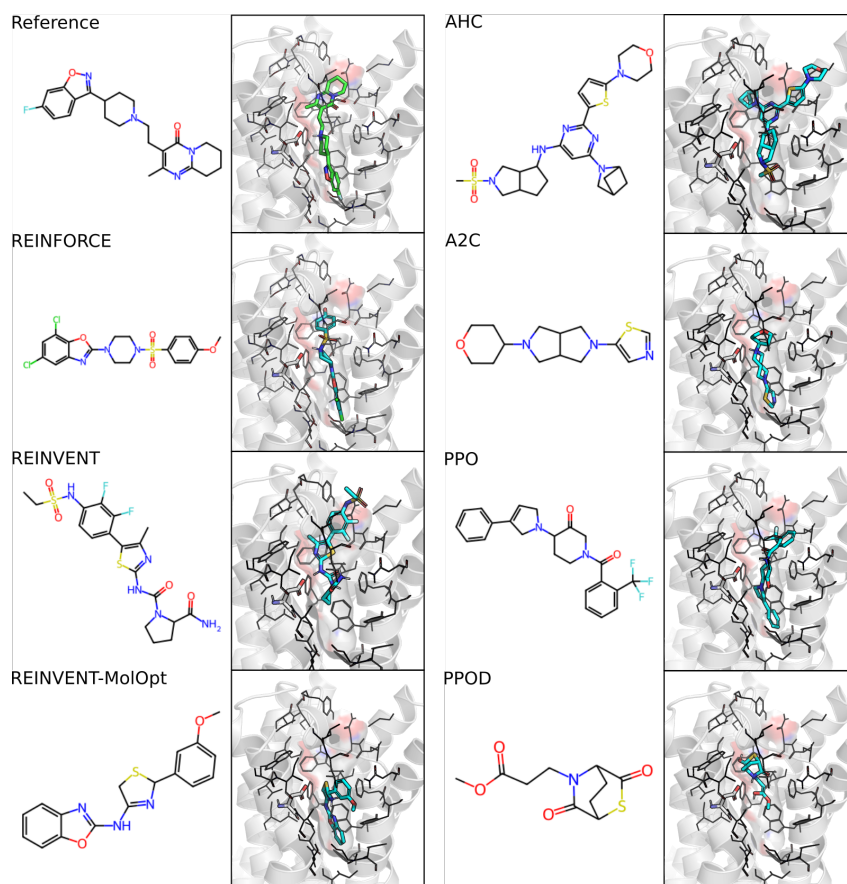


Figure 1: Selected examples from the top 10 molecules on the 5HT_{2A} selective task and their docked pose in 5-HT_{2A} (PDB: 6A93). The co-crystallised ligand Risperidone is included as the reference.

Task	Metric	ACEGEN REINFORCE	ACEGEN REINVENT	ACEGEN REINVENT-MolOpt	ACEGEN AHC	ACEGEN A2C	ACEGEN PPO	ACEGEN PPOD
D ₂	Yield	0.977	0.989	0.987	0.991	0.354	0.942	0.952
	Average score	0.679	0.720	0.743	0.794	0.723	0.749	0.760
D ₂ with reaction filters	Yield	0.972	0.992	0.988	0.990	0.555	0.950	0.947
	Average score	0.579	0.668	0.796	0.723	0.537	0.705	0.726
	Ratio of satisfied reaction filters	0.896	0.753	0.921	0.809	0.352	0.830	0.858

Table 6: Algorithm comparison in combination with PromptSMILES for constrained molecule generation on LibINVENT DRD2 tasks (without and with selective reaction filters). Each algorithm ran 5 times with different seeds, and results were averaged.

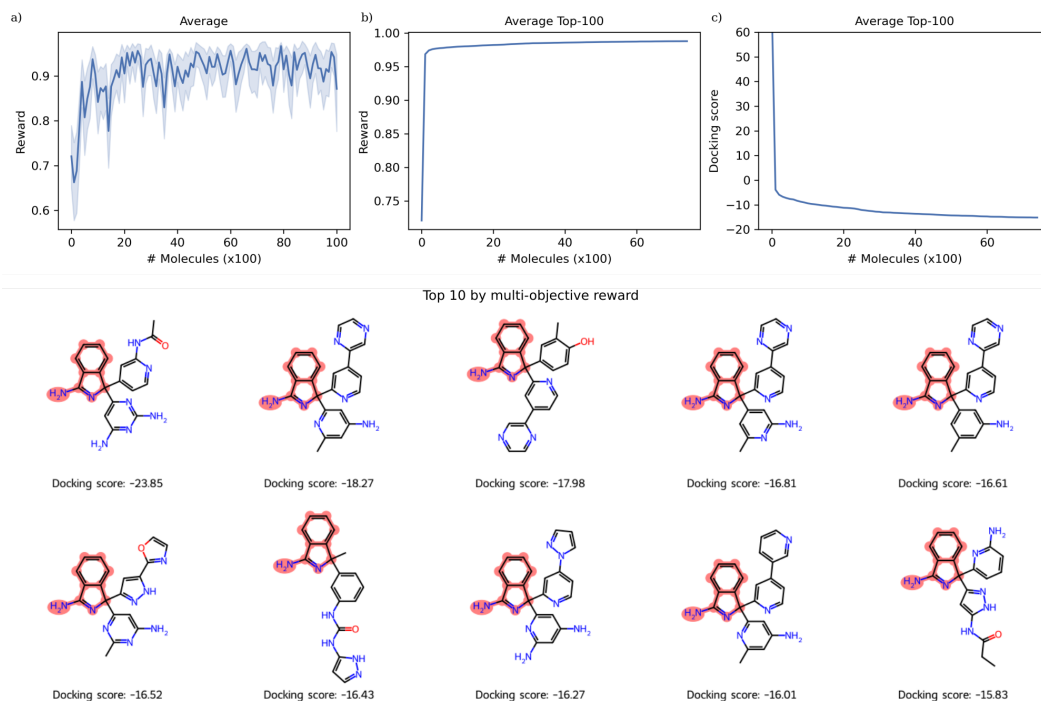


Figure 2: Optimization of the multi-objective reward. The average reward and optimization of the underlying docking score are shown. The top 10 *de novo* molecules are shown by multi-objective reward, with the constrained substructure highlighted in red and the docking score labeled below. For reference, the co-crystal ligand is re-docked with a docking score of -8.44. The docked poses are shown in Figure 15.

the P2', P1 and P3 sub-pockets Oehlrich et al. (2014). The bicyclic, amidine-containing core was used as a prompt for PromptSMILES, allowing two growth vectors, one into the P2' sub-pocket, and one into the P1 and P3 sub-pockets. Molecules were rewarded by minimizing the docking score using substructure constrained docking, as well as maintaining the number of heavy atoms and rotatable bonds in a sensible range (see Appendix F). Figure 2 shows the successful maximization of the reward over the generation of 10,000 molecules (Figure 2a,b), and corresponding minimization of the docking score (Figure 2c). The top 10 molecules identified contain improved docking scores in the range -23.9 to -15.8 compared to the reference molecule re-docked with a docking score of -8.44. Docked poses (shown in Figure 15) show the recovery of aromatic rings in the P1 and P2 sub-pockets. This case study highlights the successful constrained optimization of a complex objective.

4 CONCLUSION

In this study, we introduce ACEGEN, a novel toolkit that combines the best methodologies of reinforcement learning (RL) with the field of drug discovery. Leveraging RL building blocks from TorchRL, a general highly-tested decision-making library, ACEGEN provides modular, efficient and versatile solutions for drug discovery that we demonstrate with language-based models. We showcase ACEGEN’s capabilities across diverse areas, including method benchmarking, algorithmic exploration, and real-world drug discovery applications. Our experiments shed light on popular algorithms like REINVENT, offer practical insights into choosing the most suitable algorithm for specific contexts, and highlight the importance of dependable and comprehensive toolkits. Overall, ACEGEN addresses various needs in drug discovery and helps navigate the complex challenges associated with the field effectively.

REFERENCES

- Yuntao Bai, Andy Jones, Kamal Ndousse, Amanda Askell, Anna Chen, Nova DasSarma, Dawn Drain, Stanislav Fort, Deep Ganguli, Tom Henighan, et al. Training a helpful and harmless assistant with reinforcement learning from human feedback. *arXiv preprint arXiv:2204.05862*, 2022.
- Federico Berto, Chuanbo Hua, Junyoung Park, Minsu Kim, Hyeonah Kim, Jiwoo Son, Haeyeon Kim, Joungho Kim, and Jinkyoo Park. RL4co: an extensive reinforcement learning for combinatorial optimization benchmark. *arXiv preprint arXiv:2306.17100*, 2023.
- Thomas Blaschke, Josep Arús-Pous, Hongming Chen, Christian Margreitter, Christian Tyrchan, Ola Engkvist, Kostas Papadopoulos, and Atanas Patronov. Reinvent 2.0: an ai tool for de novo drug design. *Journal of chemical information and modeling*, 60(12):5918–5922, 2020.
- Albert Bou, Matteo Bettini, Sebastian Dittert, Vikash Kumar, Shagun Sodhani, Xiaomeng Yang, Gianni De Fabritiis, and Vincent Moens. Torchrl: A data-driven decision-making library for pytorch, 2023.
- Cédric Bouysset and Sébastien Fiorucci. Prolif: a library to encode molecular interactions as fingerprints. *Journal of cheminformatics*, 13:1–9, 2021.
- Nathan Brown, Marco Fiscato, Marwin HS Segler, and Alain C Vaucher. Guacamol: benchmarking models for de novo molecular design. *Journal of chemical information and modeling*, 59(3): 1096–1108, 2019.
- Austen B Casey, Meng Cui, Raymond G Booth, and Clinton E Canal. “selective” serotonin 5-ht2a receptor antagonists. *Biochemical pharmacology*, 200:115028, 2022.
- Kyunghyun Cho, Bart Van Merriënboer, Caglar Gulcehre, Dzmitry Bahdanau, Fethi Bougares, Holger Schwenk, and Yoshua Bengio. Learning phrase representations using rnn encoder-decoder for statistical machine translation. *arXiv preprint arXiv:1406.1078*, 2014.
- Daniel C. Elton, Zois Boukouvalas, Mark D. Fuge, and Peter W. Chung. Deep learning for molecular design—a review of the state of the art. *Mol. Syst. Des. Eng.*, 4:828–849, 2019.
- Luyu Fan, Liang Tan, Zhangcheng Chen, Jianzhong Qi, Fen Nie, Zhipu Luo, Jianjun Cheng, and Sheng Wang. Haloperidol bound d2 dopamine receptor structure inspired the discovery of subtype selective ligands. *Nature communications*, 11(1):1074, 2020.
- Vendy Fialková, Jiayi Zhao, Kostas Papadopoulos, Ola Engkvist, Esben Jannik Bjerrum, Thierry Kogej, and Atanas Patronov. Libinvent: reaction-based generative scaffold decoration for in silico library design. *Journal of Chemical Information and Modeling*, 62(9):2046–2063, 2021.
- Wenhao Gao, Tianfan Fu, Jimeng Sun, and Connor Coley. Sample efficiency matters: a benchmark for practical molecular optimization. *Advances in Neural Information Processing Systems*, 35: 21342–21357, 2022.

- Anna Gaulton, Louisa J Bellis, A Patricia Bento, Jon Chambers, Mark Davies, Anne Hersey, Yvonne Light, Shaun McGlinchey, David Michalovich, Bissan Al-Lazikani, et al. ChEMBL: a large-scale bioactivity database for drug discovery. *Nucleic acids research*, 40(D1):D1100–D1107, 2012.
- Rafael Gómez-Bombarelli, Jennifer N Wei, David Duvenaud, José Miguel Hernández-Lobato, Benjamín Sánchez-Lengeling, Dennis Sheberla, Jorge Aguilera-Iparraguirre, Timothy D Hirzel, Ryan P Adams, and Alán Aspuru-Guzik. Automatic chemical design using a data-driven continuous representation of molecules. *ACS central science*, 4(2):268–276, 2018.
- Francesca Grisoni. Chemical language models for de novo drug design: Challenges and opportunities. *Available online*, 2023:Version of Record 2 February 2023, 2023. Themed issue on Artificial Intelligence (AI) Methodology in Structural Biology; Edited by Andreas Bender, Chris de Graaf and Noel O’Boyle.
- Albert Gu and Tri Dao. Mamba: Linear-time sequence modeling with selective state spaces. *arXiv preprint arXiv:2312.00752*, 2023. doi: 10.48550/arXiv.2312.00752.
- Jeff Guo, Vendy Fialková, Juan Diego Arango, Christian Margreitter, Jon Paul Janet, Kostas Papadopoulos, Ola Engkvist, and Atanas Patronov. Improving de novo molecular design with curriculum learning. *Nature Machine Intelligence*, 4(6):555–563, 2022.
- Sepp Hochreiter and Jürgen Schmidhuber. Long short-term memory. *Neural computation*, 9(8):1735–1780, 1997.
- Fredrik Jeppsson, Susanna Eketjäll, Juliette Janson, Sofia Karlström, Susanne Gustavsson, Lise-Lotte Olsson, Ann-Cathrine Radesäter, Bart Ploeger, Gvido Cebers, Karin Kolmodin, et al. Discovery of azd3839, a potent and selective bace1 inhibitor clinical candidate for the treatment of alzheimer disease. *Journal of Biological Chemistry*, 287(49):41245–41257, 2012.
- Wengong Jin, Regina Barzilay, and Tommi Jaakkola. Junction tree variational autoencoder for molecular graph generation. In *International conference on machine learning*, pp. 2323–2332. PMLR, 2018.
- Kanako Terakado Kimura, Hidetsugu Asada, Asuka Inoue, Francois Marie Ngako Kadji, Dohyun Im, Chihiro Mori, Takatoshi Arakawa, Kunio Hirata, Yayoi Nomura, Norimichi Nomura, et al. Structures of the 5-HT_{2A} receptor in complex with the antipsychotics risperidone and zotepine. *Nature structural & molecular biology*, 26(2):121–128, 2019.
- Mario Krenn, Florian Häse, AkshatKumar Nigam, Pascal Friederich, and Alan Aspuru-Guzik. Self-referencing embedded strings (selfies): A 100 *Machine Learning: Science and Technology*, 1(4):045024, 2020. doi: 10.1088/2632-2153/aba947.
- Alex M Lamb, Anirudh Goyal ALIAS PARTH GOYAL, Ying Zhang, Saizheng Zhang, Aaron C Courville, and Yoshua Bengio. Professor forcing: A new algorithm for training recurrent networks. *Advances in neural information processing systems*, 29, 2016.
- Maxime Langevin, Rodolphe Vuilleumier, and Marc Bianciotto. Explaining and avoiding failure modes in goal-directed generation of small molecules. *Journal of Cheminformatics*, 14(1):20, 2022.
- Gabriele Libardi, Gianni De Fabritiis, and Sebastian Dittert. Guided exploration with proximal policy optimization using a single demonstration. In *International Conference on Machine Learning*, pp. 6611–6620. PMLR, 2021.
- Leland McInnes, John Healy, and James Melville. Umap: Uniform manifold approximation and projection for dimension reduction. *arXiv preprint arXiv:1802.03426*, 2018.
- Jacob Menick, Maja Trebacz, Vladimir Mikulik, John Aslanides, Francis Song, Martin Chadwick, Mia Glaese, Susannah Young, Lucy Campbell-Gillingham, Geoffrey Irving, et al. Teaching language models to support answers with verified quotes. *arXiv preprint arXiv:2203.11147*, 2022.
- Volodymyr Mnih, Adria Puigdomenech Badia, Mehdi Mirza, Alex Graves, Timothy Lillicrap, Tim Harley, David Silver, and Koray Kavukcuoglu. Asynchronous methods for deep reinforcement learning. In *International conference on machine learning*, pp. 1928–1937, 2016.

- Emmanuel Noutahi, Cristian Gabellini, Michael Craig, Jonathan SC Lim, and Prudencio Tossou. Gotta be safe: A new framework for molecular design. *Digital Discovery*, 2024.
- Noel O’Boyle and Andrew Dalke. Deepsmiles: An adaptation of smiles for use in machine-learning of chemical structures. *Working Paper*, September 19 2018. Version 1.
- Daniel Oehlrich, Hana Prokopcova, and Harrie JM Gijzen. The evolution of amidine-based brain penetrant bace1 inhibitors. *Bioorganic & medicinal chemistry letters*, 24(9):2033–2045, 2014.
- Marcus Olivecrona, Thomas Blaschke, Ola Engkvist, and Hongming Chen. Molecular de-novo design through deep reinforcement learning. *Journal of cheminformatics*, 9(1):1–14, 2017.
- Long Ouyang, Jeffrey Wu, Xu Jiang, Diogo Almeida, Carroll Wainwright, Pamela Mishkin, Chong Zhang, Sandhini Agarwal, Katarina Slama, Alex Ray, et al. Training language models to follow instructions with human feedback. *Advances in Neural Information Processing Systems*, 35: 27730–27744, 2022.
- Hakime Öztürk, Arzucan Özgür, Philippe Schwaller, Teodoro Laino, and Elif Ozkirimli. Exploring chemical space using natural language processing methodologies for drug discovery. *Drug Discovery Today*, 25(3):569–575, 2020. doi: 10.1016/j.drudis.2020.01.020.
- Adam Paszke, Sam Gross, Francisco Massa, Adam Lerer, James Bradbury, Gregory Chanan, Trevor Killeen, Zeming Lin, Natalia Gimelshein, Luca Antiga, Alban Desmaison, Andreas Kopf, Edward Yang, Zachary DeVito, Martin Raison, Alykhan Tejani, Sasank Chilamkurthy, Benoit Steiner, Lu Fang, Junjie Bai, and Soumith Chintala. PyTorch: An Imperative Style, High-Performance Deep Learning Library. In H. Wallach, H. Larochelle, A. Beygelzimer, F. d’Alché Buc, E. Fox, and R. Garnett (eds.), *Advances in Neural Information Processing Systems 32*, pp. 8024–8035. Curran Associates, Inc., 2019. URL <http://papers.neurips.cc/paper/9015-pytorch-an-imperative-style-high-performance-deep-learning-library.pdf>.
- Daniil Polykovskiy, Alexander Zhebrak, Benjamin Sanchez-Lengeling, Sergey Golovanov, Oktai Tatanov, Stanislav Belyaev, Rauf Kurbanov, Aleksey Artamonov, Vladimir Aladinskiy, Mark Veselov, et al. Molecular sets (moses): a benchmarking platform for molecular generation models. *Frontiers in pharmacology*, 11:565644, 2020.
- Mariya Popova, Olexandr Isayev, and Alexander Tropsha. Deep reinforcement learning for de novo drug design. *Science advances*, 4(7):eaap7885, 2018.
- Alec Radford, Jeffrey Wu, Rewon Child, David Luan, Dario Amodei, Ilya Sutskever, et al. Language models are unsupervised multitask learners. *OpenAI blog*, 1(8):9, 2019.
- Philipp Renz, Dries Van Rompaey, Jörg Kurt Wegner, Sepp Hochreiter, and Günter Klambauer. On failure modes in molecule generation and optimization. *Drug Discovery Today: Technologies*, 32:55–63, 2019.
- Patrick J Ropp, Jacob O Spiegel, Jennifer L Walker, Harrison Green, Guillermo A Morales, Katherine A Milliken, John J Ringe, and Jacob D Durrant. Gypsum-dl: an open-source program for preparing small-molecule libraries for structure-based virtual screening. *Journal of cheminformatics*, 11:1–13, 2019.
- Sergio Ruiz-Carmona, Daniel Alvarez-Garcia, Nicolas Foloppe, A Beatriz Garmendia-Doval, Szilveszter Juhos, Peter Schmidtke, Xavier Barril, Roderick E Hubbard, and S David Morley. rdock: a fast, versatile and open source program for docking ligands to proteins and nucleic acids. *PLoS computational biology*, 10(4):e1003571, 2014.
- Wolfgang HB Sauer and Matthias K Schwarz. Molecular shape diversity of combinatorial libraries: a prerequisite for broad bioactivity. *Journal of chemical information and computer sciences*, 43(3):987–1003, 2003.
- John Schulman, Filip Wolski, Prafulla Dhariwal, Alec Radford, and Oleg Klimov. Proximal policy optimization algorithms. *arXiv preprint arXiv:1707.06347*, 2017.

- Marwin HS Segler, Thierry Kogej, Christian Tyrchan, and Mark P Waller. Generating focused molecule libraries for drug discovery with recurrent neural networks. *ACS central science*, 4(1): 120–131, 2018.
- AN Shivanyuk, SV Ryabukhin, A Tolmachev, AV Bogolyubsky, DM Mykytenko, AA Chupryna, W Heilman, and AN Kostyuk. Enamine real database: Making chemical diversity real. *Chemistry today*, 25(6):58–59, 2007.
- Richard S Sutton and Andrew G Barto. *Reinforcement learning: An introduction*. MIT press, 2018.
- Morgan Thomas, Robert T Smith, Noel M O’Boyle, Chris de Graaf, and Andreas Bender. Comparison of structure-and ligand-based scoring functions for deep generative models: a gpcc case study. *Journal of cheminformatics*, 13(1):1–20, 2021.
- Morgan Thomas, Noel M O’Boyle, Andreas Bender, and Chris De Graaf. Augmented hill-climb increases reinforcement learning efficiency for language-based de novo molecule generation. *Journal of Cheminformatics*, 14(1):1–22, 2022.
- Morgan Thomas, Noel M O’Boyle, Andreas Bender, and Chris De Graaf. Molscore: A scoring and evaluation framework for de novo drug design. 2023.
- Morgan Thomas, Mazen Ahmad, Gary Tresadern, and Gianni de Fabritiis. Promptsmls: Prompting for scaffold decoration and fragment linking in chemical language models. 2024.
- Hugo Touvron, Louis Martin, Kevin Stone, Peter Albert, Amjad Almahairi, Yasmine Babaei, Nikolay Bashlykov, Soumya Batra, Prajjwal Bhargava, Shruti Bhosale, et al. Llama 2: Open foundation and fine-tuned chat models. *arXiv preprint arXiv:2307.09288*, 2023. doi: 10.48550/arXiv.2307.09288.
- Umit V Ucak, Islambek Ashyrmamatov, and Juyong Lee. Improving the quality of chemical language model outcomes with atom-in-smiles tokenization. *Journal of cheminformatics*, 15(1):55, 2023.
- Mingyang Wang, Zhe Wang, Huiyong Sun, Jike Wang, Chao Shen, Gaoqi Weng, Xin Chai, Honglin Li, Dongsheng Cao, and Tingjun Hou. Deep learning approaches for de novo drug design: An overview. *Current Opinion in Structural Biology*, 72:135–144, 2022.
- Sheng Wang, Tao Che, Anat Levit, Brian K Shoichet, Daniel Wacker, and Bryan L Roth. Structure of the d2 dopamine receptor bound to the atypical antipsychotic drug risperidone. *Nature*, 555(7695):269–273, 2018.
- David Weininger. Smiles, a chemical language and information system. 1. introduction to methodology and encoding rules. *Journal of chemical information and computer sciences*, 28(1):31–36, 1988.
- Ronald J Williams. Simple statistical gradient-following algorithms for connectionist reinforcement learning. *Machine learning*, 8:229–256, 1992.
- William J. Wiswesser. Historic development of chemical notations. *Journal of Chemical Information and Computer Sciences*, 25(3):258–263, 1985. doi: 10.1021/ci00047a023.
- Botian Xu, Feng Gao, Chao Yu, Ruize Zhang, Yi Wu, and Yu Wang. Omnidrones: An efficient and flexible platform for reinforcement learning in drone control. *IEEE Robotics and Automation Letters*, 2024.

APPENDIX

A REINFORCEMENT LEARNING ENVIRONMENT

```

1 from acegen.rl_env import SMILESEnv
2 from acegen.vocabulary import SMILESVocabulary
3 from torchrl.collectors import RandomPolicy
4
5 # Create a vocabulary from a list of characters
6 chars = ["START", "END", "(", ")", "1", "=", "C", "N", "O"]
7 chars_dict = {char: index for index, char in enumerate(chars)}
8 vocab = SMILESVocabulary.create_from_dict(chars_dict, start_token="START"
9     , end_token="END")
10
11 # Create an environment from the vocabulary
12 env = SMILESEnv(
13     start_token=vocab.start_token_index,
14     end_token=vocab.end_token_index,
15     length_vocabulary=len(vocab),
16     batch_size=4, # Number of trajectories to collect in parallel
17 )
18 # Create a random policy
19 policy = RandomPolicy(env.full_action_spec)
20
21 # Take an environment step
22 step_tensordict = env.step(policy(env.reset()))
23 print(step_tensordict)

```

Output:

```

TensorDict(
  fields={
    action: Tensor(shape=torch.Size([4]), device=cpu, dtype=torch.int32,
    done: Tensor(shape=torch.Size([4, 1]), device=cpu, dtype=torch.bool),
    next: TensorDict(
      fields={
        done: Tensor(shape=torch.Size([4, 1]), device=cpu, dtype=torch.bool),
        observation: Tensor(shape=torch.Size([4]), device=cpu, dtype=torch.int64),
        reward: Tensor(shape=torch.Size([4, 1]), device=cpu, dtype=torch.float32),
        terminated: Tensor(shape=torch.Size([4, 1]), device=cpu, dtype=torch.bool),
        truncated: Tensor(shape=torch.Size([4, 1]), device=cpu, dtype=torch.bool)},
        batch_size=torch.Size([4]),
        device=cpu,
        is_shared=False),
    observation: Tensor(shape=torch.Size([4]), device=cpu, dtype=torch.int32),
    terminated: Tensor(shape=torch.Size([4, 1]), device=cpu, dtype=torch.bool),
    truncated: Tensor(shape=torch.Size([4, 1]), device=cpu, dtype=torch.bool)},
    batch_size=torch.Size([4]),
    device=cpu,
    is_shared=False)

```

Figure 3: Code example that shows how to create a language-based reinforcement learning environment components for SMILES generation and how to take sampling steps on it with a random policy.

B DEFINE SCORING FUNCTIONS

```

1 from molscore.manager import MolScore
2
3 task = MolScore(
4     model_name="example",
5     task_config=path/to/molscore/config/MolOpt/Albyterol_similarity.json,
6     budget=10,
7     output_dir="/tmp",
8 )
9
10 env = SMILESEnv(
11     start_token=vocab.start_token_index,
12     end_token=vocab.end_token_index,
13     length_vocabulary=len(vocab),
14     batch_size=1,
15 )
16
17 data = env.rollout(max_steps=100)
18 smiles_str = [vocab.decode(smi.numpy()) for smi in data["action"]]
19 reward = task(smiles_str)

```

Figure 4: An example scoring function created using MolScore.

```

1 from rdkit.Chem import AllChem, QED
2
3 def evaluate_mol(smiles: str):
4     mol = AllChem.MolFromSmiles(smiles)
5     if mol:
6         return QED(mol)
7     else:
8         return 0.0
9
10 def evaluate_mols(smiles: list):
11     return [evaluate_mol(smi) for smi in smiles]
12
13 env = SMILESEnv(
14     start_token=vocab.start_token_index,
15     end_token=vocab.end_token_index,
16     length_vocabulary=len(vocab),
17     batch_size=1,
18 )
19
20 data = env.rollout(max_steps=100)
21 smiles_str = [vocab.decode(smi.numpy()) for smi in data["action"]]
22 reward = evaluate_mols(smiles_str)

```

Figure 5: An example of custom scoring function that returns a reward based on an input molecule. If the molecule is invalid, no reward is returned (i.e., 0.0).

C COMPARISON AGAINST AN EXISTING IMPLEMENTATION

We conducted a comparative analysis between our Reinvent implementation and MolOpt’s (Guo et al., 2022) implementation, which is accessible on their Github repository. To ensure a fair comparison, we replaced only the prior weights and utilized MolScore for computing scoring functions. Apart from these adjustments, we maintained the use of the original code. Both implementations use the same network architecture and hyperparameters.

Table 7 and Table 8 show that our code is faster and obtains higher values for all metrics with compared to that implementation. The observed performance gaps may stem from subtle idiosyncrasies within the codebase. In reinforcement learning, even minor variations can yield notable discrepancies in outcomes. This underscores the importance of employing standardized, rigorously tested components and foundational building blocks, which offer heightened reliability. Furthermore, we hypothesize the enhanced efficiency can be attributed to leveraging components from TorchRL, a part of the META ecosystem, which inherently provides better optimization and reliability compared to bespoke solutions.

Task	REINVENT MolOpt Implementation	REINVENT ACEGEN Implementation
Albuterol similarity	2:06 mins	1:01 mins
Amlodipine MPO	5:05 mins	3:25 mins
C7H8N2O2	1:44 mins	0:42 mins
C9H10N2O2PF2Cl	1:44 mins	0:37 mins

Table 7: Comparison of REINVENT MolOpt Implementation and REINVENT ACEGEN Implementation code on a machine with 32 CPUs and a NVIDIA GeForce RTX 4090 GPU for different scoring functions. In each run the algorithm generates and trains on 10K molecules.

Metric	REINVENT MolOpt Implementation	REINVENT ACEGEN Implementation
Avg top 10	15.833	15.959
Avg top 100	14.640	14.896
AUC top 10	13.597	13.740
AUC top 100	11.873	11.985

Table 8: Comparison of REINVENT MolOpt Implementation and ACEGEN AceGen Implementation on the MolOpt benchmark scoring functions. The results are presented as the sum of all scoring function in the benchmark for different metrics. Each algorithm ran 5 times with different seeds, and results were averaged.

D MOLOPT BENCHMARK

The MolOpt benchmark was run using the MolScore implementation for convenience as it automatically calculates the same metrics as in the original implementation. In addition, MolScore computes the metrics after the removal of undesirable chemistry via the use of a basic chemistry filter (B-CF). This filter ensures molecules have a logP less than or equal to 4.5, rotatable bond count less than or equal to 7, molecular weight in the range 150 to 650 Da, only contain atoms belonging to the following set $A \in \{C, S, O, N, H, F, Cl, Br\}$, and do not violate the substructure alerts as described in Polykovskiy et al. (2020). If provided with a set of reference molecules, MolScore computes the metrics after the remove of undesirable chemistry via the use of a target chemistry filter (T-CF). This filter ensures molecules have a molecular weight and logP range within $\mu \pm 4\sigma$ of the reference distribution, as well as, removing any molecule that comprises $> 10\%$ novel atomic environment bits with respect to the reference molecules, as measured by ECFP4 bits (an example of this is shown in Figure 8). Lastly, MolScore also computes the metrics after filtering molecules using both basic and target chemistry filters (B&T-CF).

Metric	AceGen REINFORCE	AceGen REINVENT	AceGen REINVENT-MolOpt	AceGen AHC	AceGen A2C	AceGen PPO	AceGen PPOD
Valid	21.77	21.78	21.74	21.45	18.93	textbf21.78	21.52
Top-1 Avg	16.60	16.41	17.73	16.77	16.35	16.14	17.47
Top-10 Avg	15.85	15.69	17.43	16.09	15.67	15.63	17.10
Top-100 Avg	14.59	14.41	16.90	14.95	14.66	14.81	16.50
Top-1 AUC	14.85	14.79	16.28	15.06	15.21	15.39	16.41
Top-10 AUC	13.67	13.60	15.65	13.91	14.27	14.65	15.80
Top-100 AUC	11.96	11.84	14.58	12.17	12.83	13.41	14.67
Top-1 Avg (Div)	16.60	16.41	17.73	16.77	16.35	16.14	17.47
Top-10 Avg (Div)	15.63	15.46	17.13	15.90	15.42	15.35	16.70
Top-100 Avg (Div)	13.89	13.76	14.62	14.21	13.68	12.63	13.54
Top-1 AUC (Div)	14.85	14.79	16.28	15.06	15.21	15.39	16.41
Top-10 AUC (Div)	13.53	13.47	15.42	13.76	14.09	14.37	15.39
Top-100 AUC (Div)	11.66	11.56	13.07	11.80	12.26	11.67	12.36
Unique	22.28	22.63	13.68	22.68	18.38	9.47	10.21
B&T-CF	14.34	14.74	7.00	13.77	7.82	5.81	5.71
B&T-CF Top-1 Avg	15.97	15.86	16.85	16.13	15.61	15.52	16.69
B&T-CF Top-10 Avg	15.21	15.07	16.44	15.44	14.83	14.99	16.32
B&T-CF Top-100 Avg	13.75	13.68	15.61	14.18	13.54	13.98	15.46
B&T-CF Top-1 AUC	14.26	14.20	15.60	14.47	14.54	14.81	15.74
B&T-CF Top-10 AUC	13.06	12.98	14.91	13.27	13.52	14.02	15.11
B&T-CF Top-100 AUC	11.24	11.15	13.61	11.44	11.88	12.64	13.76
B&T-CF Top-1 Avg (Div)	15.97	15.86	16.85	16.13	15.61	15.52	16.69
B&T-CF Top-10 Avg (Div)	14.95	14.83	16.06	15.25	14.54	14.60	15.78
B&T-CF Top-100 Avg (Div)	12.96	12.95	13.12	13.31	12.44	11.41	12.14
B&T-CF Top-1 AUC (Div)	14.26	14.20	15.60	14.47	14.54	14.81	15.74
B&T-CF Top-10 AUC (Div)	12.91	12.85	14.61	13.11	13.32	13.67	14.60
B&T-CF Top-100 AUC (Div)	10.91	10.84	11.84	11.04	11.21	10.59	11.19
B&T-CF Diversity (SEDiv@1k)	17.39	18.19	10.10	17.55	14.24	8.47	7.96

Table 9: Performance summary of algorithms for further metrics measured in this benchmark. Each algorithm ran 5 times with different seeds, and results were averaged and then summed over tasks.

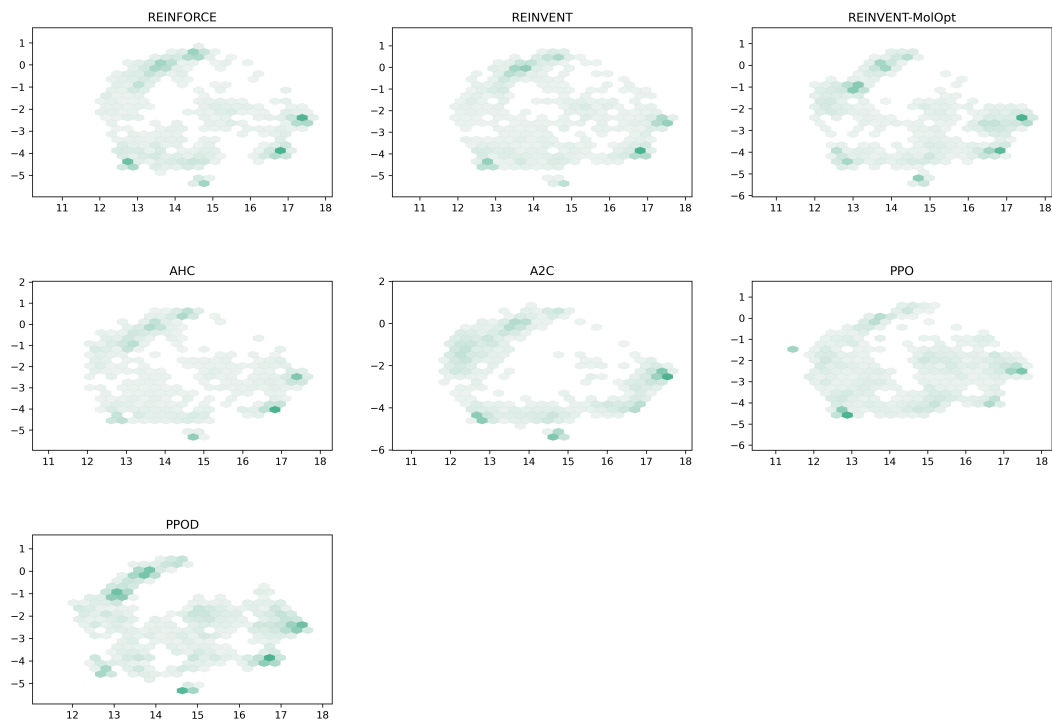


Figure 6: Visualization of the chemical space of the top 100 molecules across all tasks and repetitions by RL algorithm.

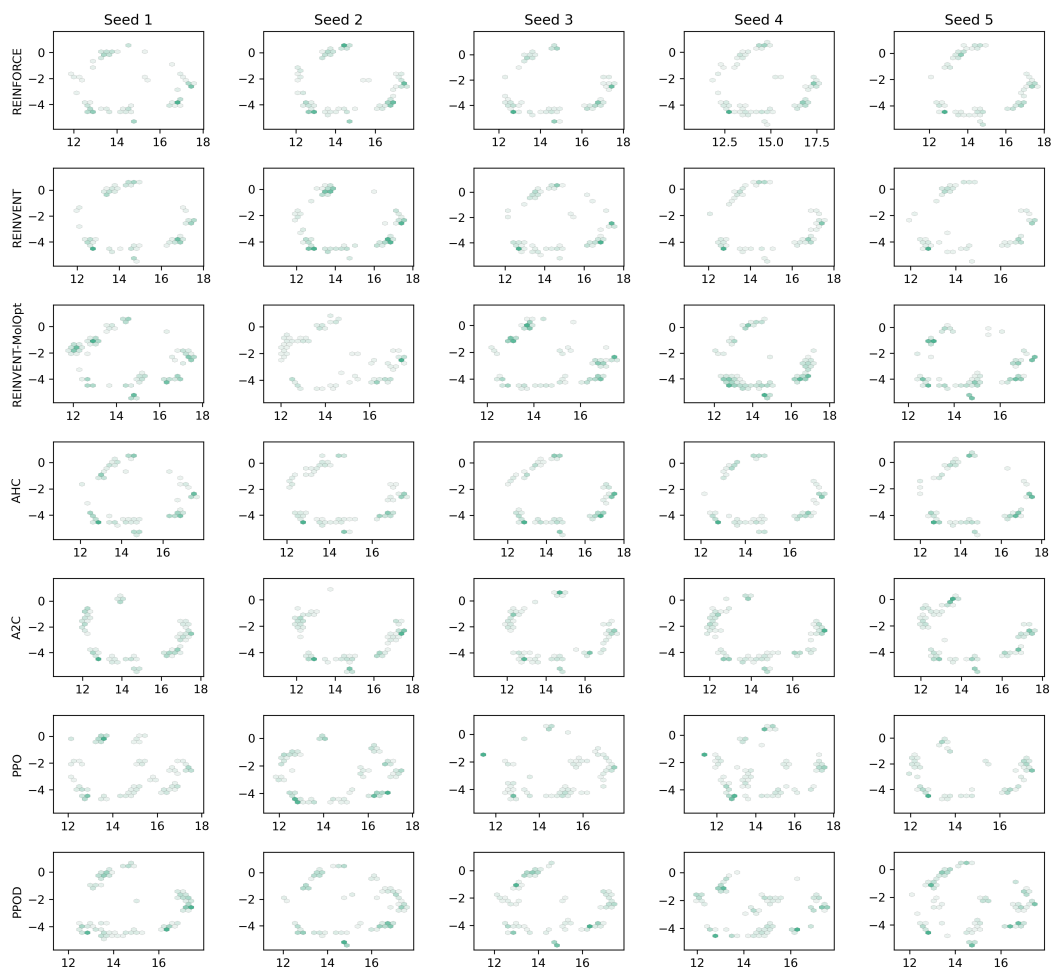


Figure 7: Visualization of the consistency of chemical space of the top 100 molecules across all tasks by repetition and RL algorithm.

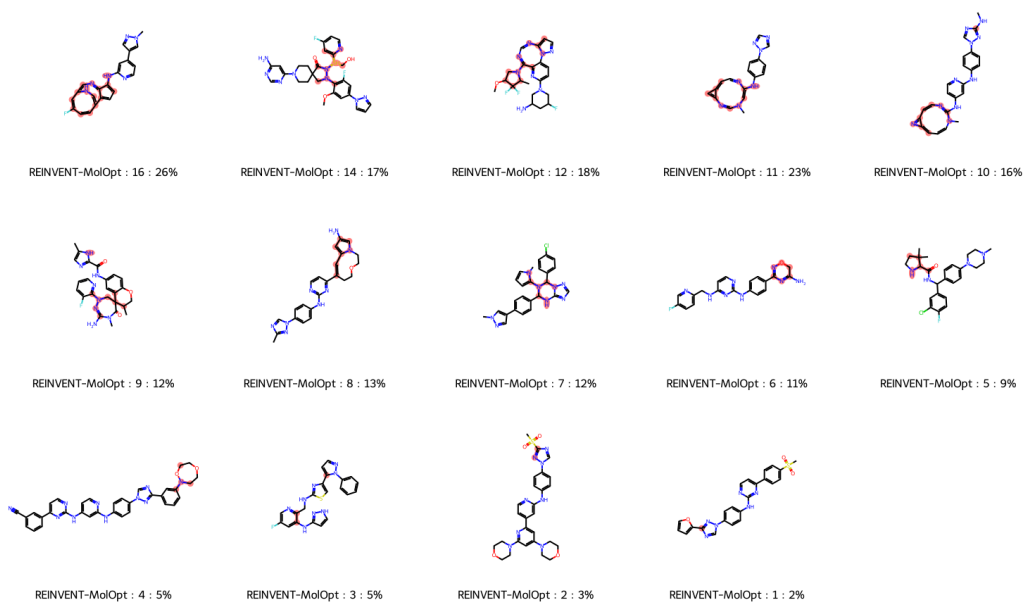


Figure 8: Demonstration of molecules measured as idiosyncratic by their percentage of novel ECFP4 bits relative to a reference dataset, with novel bits highlighted in red. Molecules are taken from those generated on the JNK3 task and are labelled by RL algorithm, number of novel bits, and percentage of novel bits relative to all bits present in the molecule.

E 5-HT_{2A} CASE STUDY

The same training dataset and pre-trained prior was used as for the MolOpt benchmark. For the docking objectives, PDB structures 6A93 Kimura et al. (2019) and 6CM4 Wang et al. (2018) were used for 5-HT_{2A} the D₂ respectively. For further details of docking protocol see MolScore Thomas et al. (2023) and a configuration file to reproduce the objective can be found at <https://github.com/MorganCThomas/MolScore/>. The score for each molecule is in the range [0-1] and is calculated as a weighted sum of the individual scoring components described in Table 10. Note that during training, the inter-molecular rDock score was used as it was otherwise observed that RL would hack score optimization by improvement of intra-molecular rDock score only (data not shown). To discourage excessive exploitation, a diversity filter was used to penalize the re-use scaffolds similar to those previously sampled. The 126 known 5-HT_{2A} ligands were extracted from ChEMBL31 and contained a pChEMBL_{5-HT_{2A}} bioactivity value ≥ 6 and displayed atleast 100-fold selectivity versus D₂ (pChEMBL_{5-HT_{2A}} - pChEMBL_{D₂} ≥ 2). All metrics calculated during analysis were calculated using MolScore. Uniform manifold approximation and projection (UMAP) McInnes et al. (2018) was used to visualize chemical space, calculated using Jaccard distance with a minimum similarity of 0.1 and number of neighbours of 100 on ECFP6 fingerprints. The UMAP was fit to a random subset of 10,000 molecules taken from the prior training dataset. Normalized principal moments Sauer & Schwarz (2003) were calculated using RDKit on the docked poses to visualize molecular geometry. Protein-ligand interaction fingerprints were calculated on docked poses using the ProLIF library Bouysset & Fiorucci (2021).

To further probe the differences in the chemistry proposed by the different RL algorithms, the metrics were calculated on all generated *de novo* molecules within the budget, shown in Tables 12, 13, and 14. Notably, ACEGEN-REINVENT-MolOpt achieved the best average 100 score but performed poorly with respect to chemistry-related metrics such as the ratio of molecules passing quality filters, chemical diversity and idiosyncratic atomic environments as measured by outlier bits with respect to the pre-training dataset. Other algorithms such as, ACEGEN-REINVENT with default parameters, AHC, PPO, and PPOD perform better in these chemistry-related metrics, suggesting an overall higher quality of chemistry proposed. This could reflect stronger regularisation towards the prior distribution, confirmed by higher similarity to the initial pre-training dataset (Table 13). In comparison to the extracted set of known 5-HT_{2A} ligands (Table 14), ACEGEN-AHC manages to generate at least one analog to 78% of known ligands, followed by ACEGEN-REINVENT at 63% and then PPOD at 55%. A visualization of the chemical space explored is shown in 10, showing that ACEGEN-REINFORCE and ACEGEN-REINVENT are most explorative, followed by ACEGEN-AHC, ACEGEN-A2C, ACEGEN-PPO, REINVENT-MolOpt and finally ACEGEN-PPOD least explorative. This results in complementary chemical space occupation of the top 100 solutions by either algorithm (Figure 11), all of which show areas of overlap with the known 5-HT_{2A} ligands. Interestingly, a number of the example molecules (Figure 12) contain caged sub-structures or macrocycles typically observed more frequently in natural products than typical small-molecule drugs. This could be a result of the selectivity required in the objective, where more 3D spherical structures are typically more specific binders, but are more challenging synthetically. This can also be seen by a slight shift towards spherical geometries by the ACEGEN-A2C and ACEGEN-PPOD compounds compared to the known selective ligands, shown in Figure 13.

A comparison of the protein interactions made by the top 10 compounds highlight the targeting of potentially selectivity inducing interactions. Figure 14 shows that many of the top 10 compounds proposed by ACEGEN-REINFORCE and ACEGEN-AHC form interactions with S131, T134, W151, and I152 in the second extended binding pocket which differ to those found in D₂, and therefore, could potentially be a site to obtain selectivity. For example, occupied by the caged substructure shown in the selected examples in Figure 1 proposed by ACEGEN-AHC, occupying a sub-pocket that is not sterically possible in the D₂ crystal structure used here. However, other D₂ structures do show occupation of this after re-arrangement of extracellular loop 1 Fan et al. (2020). This reinforces the difficulty in identifying robust, validated scoring functions or oracles in drug discovery. For example, the use of Gypsum-DL Ropp et al. (2019) to prepare ligands for docking in this protocol leads to the generation of some implausible tautomers and unlikely protonation states and geometries (for example, cis-amides), meanwhile the docking parameters need further refinement to improve the quality of binding poses and cationic interactions with D155^{3x32} which are sometimes in an unlikely orientation. These can be swapped for commercial products like LigPrep in MolScore provided the licence is obtained. However, this challenging objective enables the differentiation of

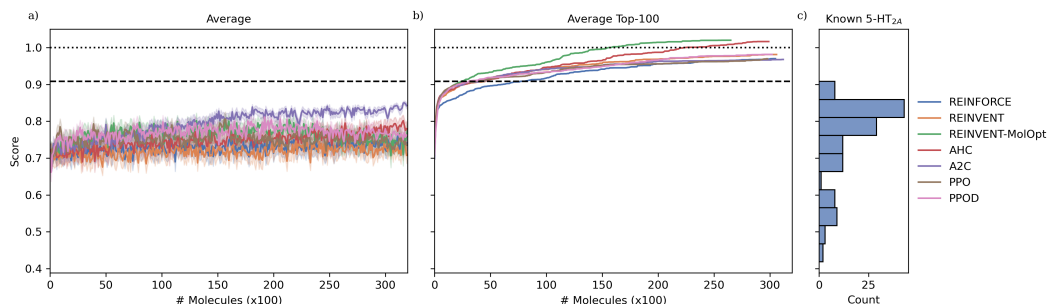


Figure 9: Optimisation of a challenging 5-HT_{2A} structure-based selectivity objective by different RL algorithms. The average score does not improve much over the course of training, but the average score of the top 100 compounds improves beyond known selective 5-HT_{2A} ligands. Note that the values here are re-normalized based on the scores achieved for a subset of 5-HT_{2A} ligands that display at least 2-fold selectivity over D₂ as extracted from ChEMBL31 Gaulton et al. (2012). Therefore, a score of 0.91 indicates the best score observed in the known ligand subset, and a score greater than 1.0 indicates that a single molecule achieves both a better (more negative) 5-HT_{2A} docking score and (more positive) D₂ docking score than seen anywhere in the known subset.

RL performance and behaviour in the optimization of a specified objective and sets a realistic and practical benchmark for drug discovery.

Scoring function	Comments	Target	Weight
5-HT _{2A} docking score (inter-molecular only)	<ul style="list-style-type: none"> - Positional cationic restraint for D^{3x:32} - Best score of any protonated/tautomerised/isomeric variant - Normalized based on maximum/minimum values observed at timestep 	Minimize	1
D ₂ docking score (inter-molecular only)	<ul style="list-style-type: none"> - Best score of any protonated/tautomerised/isomeric variant - Normalized based on maximum/minimum values observed at timestep 	Maximize	0.5
Net positive charge		1	1
Maximum number of consecutive rotatable bonds		≤ 3	1

Table 10: Description of the scoring functions to define the 5-HT_{2A} selective objective.

Metric	ACEGEN REINFORCE	ACEGEN REINVENT	ACEGEN REINVENT-MolOpt	ACEGEN AHC	ACEGEN A2C	ACEGEN PPO	ACEGEN PPOD
Valid	0.95	0.96	0.93	0.94	0.98	0.94	0.95
Top-1 Avg	1.14	1.15	1.20	1.15	1.11	1.09	1.10
Top-10 Avg	1.05	1.09	1.10	1.10	1.04	1.06	1.07
Top-100 Avg	0.97	0.98	1.02	1.02	0.97	0.97	0.98
Top-1 AUC	1.10	1.12	1.12	1.12	1.09	1.06	1.08
Top-10 AUC	1.02	1.05	1.05	1.05	1.02	1.01	1.02
Top-100 AUC	0.93	0.95	0.97	0.96	0.94	0.94	0.94
Top-1 Avg (Div)	1.14	1.15	1.20	1.15	1.11	1.09	1.10
Top-10 Avg (Div)	1.05	1.08	1.10	1.10	1.04	1.06	1.07
Top-100 Avg (Div)	0.97	0.98	1.01	1.02	0.97	0.97	0.98
Top-1 AUC (Div)	1.10	1.12	1.12	1.12	1.09	1.06	1.08
Top-10 AUC (Div)	1.02	1.05	1.05	1.05	1.02	1.01	1.02
Top-100 AUC (Div)	0.93	0.95	0.96	0.96	0.94	0.93	0.94
Unique	1.00	1.00	0.89	1.00	1.00	0.99	0.99
B&T-CF	0.71	0.71	0.45	0.63	0.27	0.59	0.48
B&T-CF Top-1 Avg	1.14	1.13	1.12	1.15	1.11	1.08	1.10
B&T-CF Top-10 Avg	1.05	1.07	1.08	1.10	1.02	1.02	1.03
B&T-CF Top-100 Avg	0.96	0.97	1.00	1.00	0.93	0.95	0.96
B&T-CF Top-1 AUC	1.10	1.11	1.08	1.12	1.09	1.03	1.08
B&T-CF Top-10 AUC	1.01	1.03	1.04	1.05	1.01	0.99	0.99
B&T-CF Top-100 AUC	0.92	0.94	0.96	0.95	0.92	0.93	0.93
B&T-CF Top-1 Avg (Div)	1.14	1.13	1.12	1.15	1.11	1.08	1.10
B&T-CF Top-10 Avg (Div)	1.05	1.06	1.08	1.10	1.02	1.02	1.03
B&T-CF Top-100 Avg (Div)	0.95	0.97	0.98	1.00	0.93	0.95	0.95
B&T-CF Top-1 AUC (Div)	1.10	1.11	1.08	1.12	1.09	1.03	1.08
B&T-CF Top-10 AUC (Div)	1.01	1.03	1.04	1.05	1.00	0.99	0.99
B&T-CF Top-100 AUC (Div)	0.92	0.93	0.94	0.95	0.92	0.92	0.92
B&T-CF Diversity (SEDiv@1k)	0.89	0.91	0.64	0.89	0.77	0.60	0.53

Table 11: Performance summary of algorithms for average top-n metrics on 5-HT_{2A} case study. Including after applying a basic chemistry filter (B-CF) as described previously. B-CF is the fraction of molecules that pass the chemistry filter.

Metric	ACEGEN REINFORCE	ACEGEN REINVENT	ACEGEN REINVENT-MolOpt	ACEGEN AHC	ACEGEN A2C	ACEGEN PPO	ACEGEN PPOD
Validity	0.95	0.96	0.93	0.94	0.98	0.94	0.95
Uniqueness	1.00	1.00	0.89	1.00	1.00	0.99	0.99
Scaffold Uniqueness	0.91	0.90	0.76	0.95	0.98	0.80	0.84
Novelty	1.00	0.99	1.00	1.00	1.00	1.00	1.00
IntDiv	0.87	0.87	0.85	0.86	0.86	0.85	0.83
ScaffDiv	0.85	0.85	0.82	0.85	0.85	0.82	0.81
SEDiv@1k	0.89	0.93	0.64	0.92	0.58	0.70	0.61
SPDiv@1k	0.89	0.89	0.87	0.89	0.87	0.87	0.86
FG	0.02	0.02	0.01	0.03	0.01	0.04	0.05
RS	0.04	0.04	0.03	0.05	0.04	0.02	0.02
Quality Filters	0.85	0.84	0.70	0.84	0.56	0.84	0.78
Predicted Purchasability	0.01	0.02	0.01	0.01	0.01	0.02	0.01

Table 12: Summary of metrics measuring intrinsic properties of the chemistry generated by different algorithms. Most metrics are different measures of chemical diversity, therefore, higher is generally better but can sometimes be a result of idiosyncratic chemistry.

Metric	ACEGEN REINFORCE	ACEGEN REINVENT	ACEGEN REINVENT-MolOpt	ACEGEN AHC	ACEGEN A2C	ACEGEN PPO	ACEGEN PPOD
Analogue Similarity	0.28	0.27	0.09	0.21	0.05	0.21	0.22
Analogue Coverage	0.52	0.54	0.21	0.44	0.23	0.27	0.25
FG	0.96	0.98	0.68	0.91	0.69	0.90	0.66
RS	1.00	1.00	0.96	0.98	0.46	0.97	0.97
SNN	0.37	0.37	0.33	0.36	0.27	0.36	0.36
Frag	0.97	0.98	0.89	0.94	0.42	0.96	0.90
Scaf	0.30	0.34	0.07	0.19	0.07	0.14	0.11
OutlierBits	0.08	0.08	0.12	0.10	0.21	0.11	0.12

Table 13: Summary of metrics measuring extrinsic properties of the chemistry generated by different algorithms with respect to the initial training dataset. Metrics are different measures of chemical similarity, therefore, higher is generally better (with the exception of OutlierBits) depending on how much it is desirable to regularize the model and maintain initial prior biases.

Metric	ACEGEN	ACEGEN	ACEGEN	ACEGEN	ACEGEN	ACEGEN	ACEGEN
	REINFORCE	REINVENT	REINVENT-MolOpt	AHC	A2C	PPO	PPOD
Analogue Similarity	0.01	0.00	0.00	0.00	0.00	0.00	0.01
Analogue Coverage	0.64	0.63	0.39	0.78	0.13	0.25	0.55
FG	0.66	0.65	0.59	0.65	0.42	0.62	0.59
RS	0.75	0.74	0.72	0.73	0.30	0.71	0.76
SNN	0.23	0.22	0.23	0.22	0.18	0.24	0.24
Frag	0.52	0.51	0.59	0.50	0.10	0.50	0.46
Scaf	0.00	0.00	0.00	0.00	0.00	0.00	0.00
OutlierBits	0.41	0.42	0.40	0.43	0.52	0.38	0.39

Table 14: Summary of metrics measuring extrinsic properties of the chemistry generated by different algorithms with respect to known 5-HT_{2A} ligands. Metrics are different measures of chemical similarity, therefore, higher is generally better (with the exception of OutlierBits) depending on how much it is desirable to rediscover known chemistry.

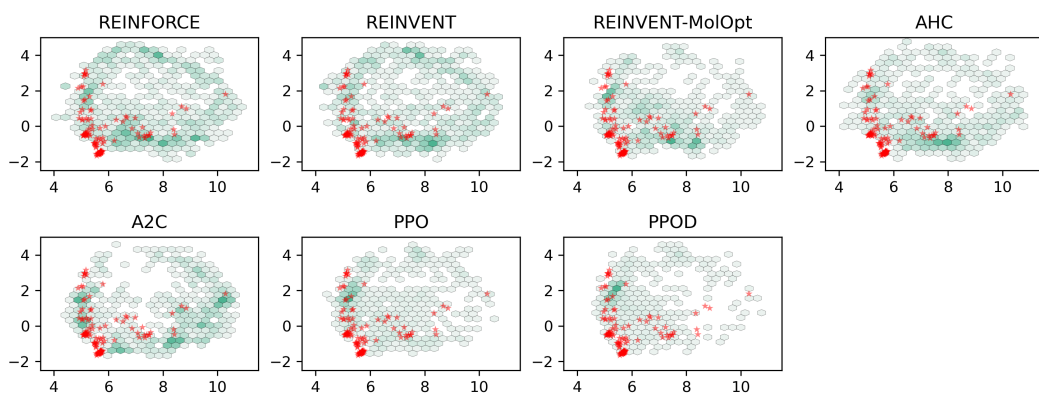


Figure 10: Chemical space explored by different RL algorithms as visualized by UMAP embedding. Known 5-HT_{2A} ligands are plotted in red.

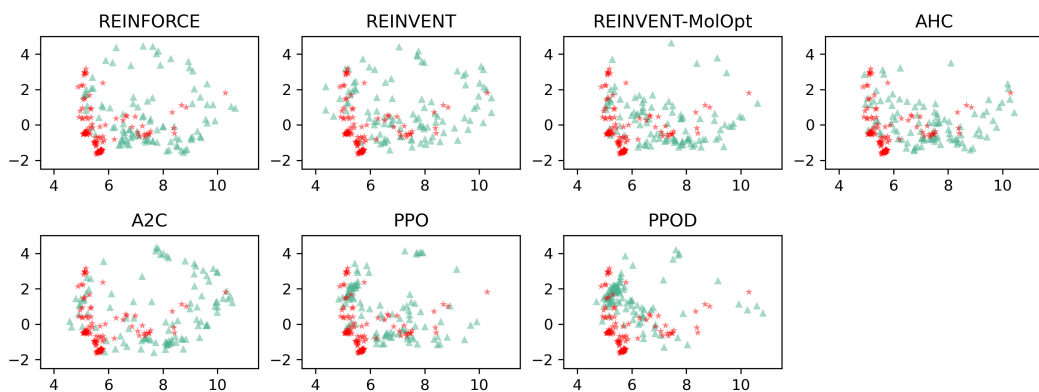


Figure 11: Chemical space of the top 100 molecules identified by each RL algorithms as visualized by UMAP embedding. Known 5-HT_{2A} ligands are plotted in red.

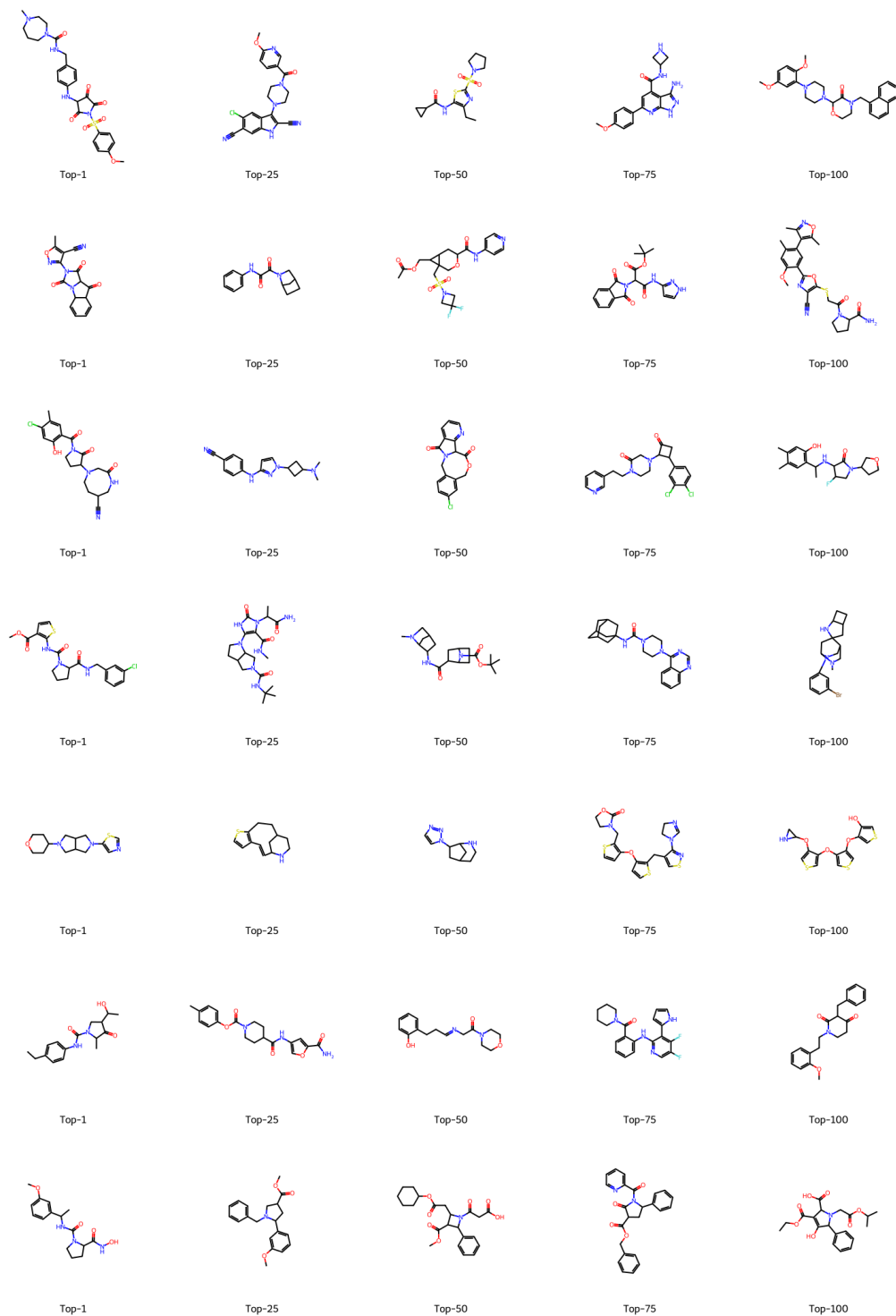


Figure 12: Five example molecules in the range of the top 100 by score. Each row represents REINFORCE, REINVENT, REINVENT-MolOpt, AHC, A2C, PPO and PPOD respectively.

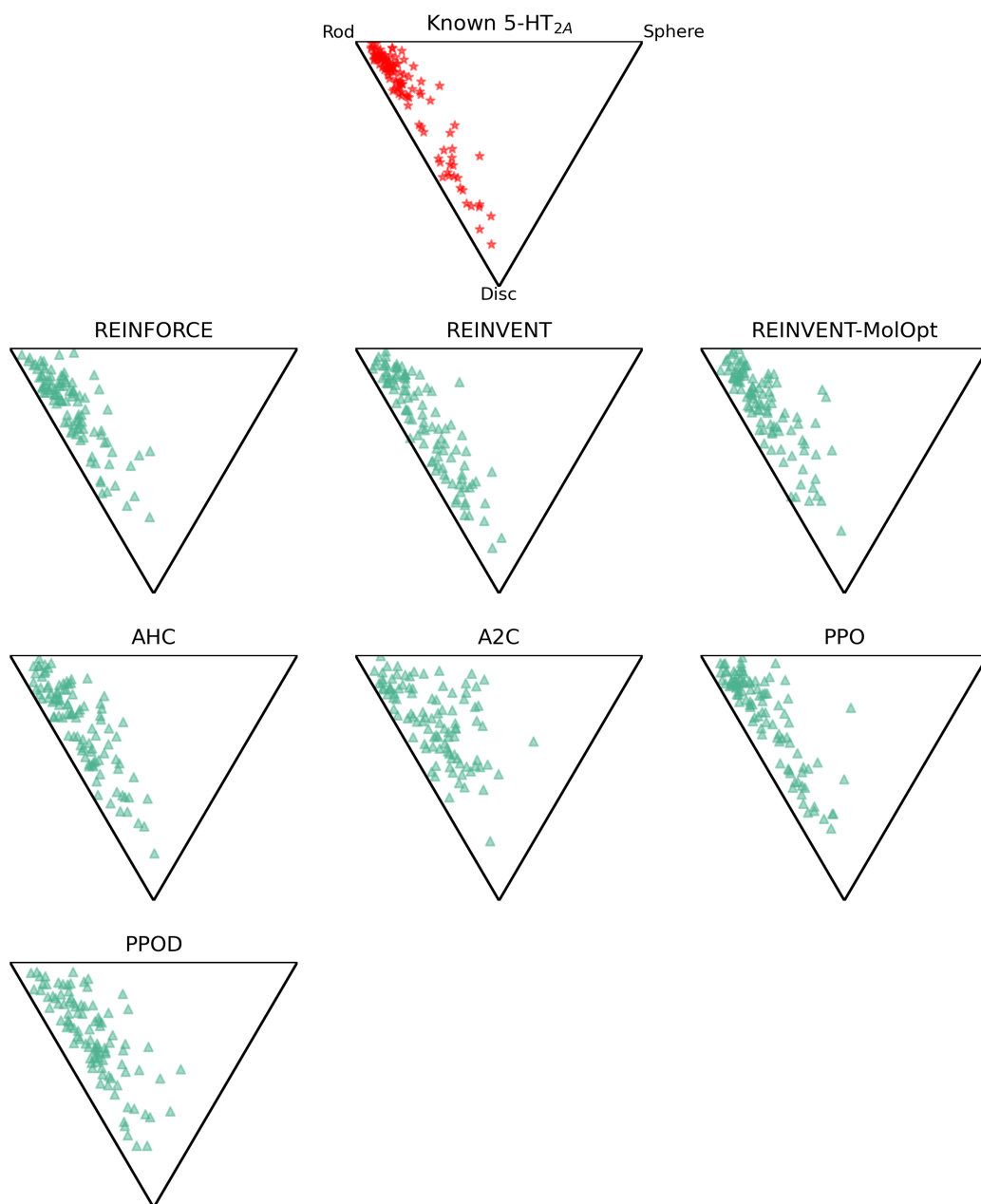


Figure 13: Normalized principal moment ratio space measuring the 3D geometrical shape of the known 5-HT_{2A} ligands and top 100 from generated by the RL algorithms.

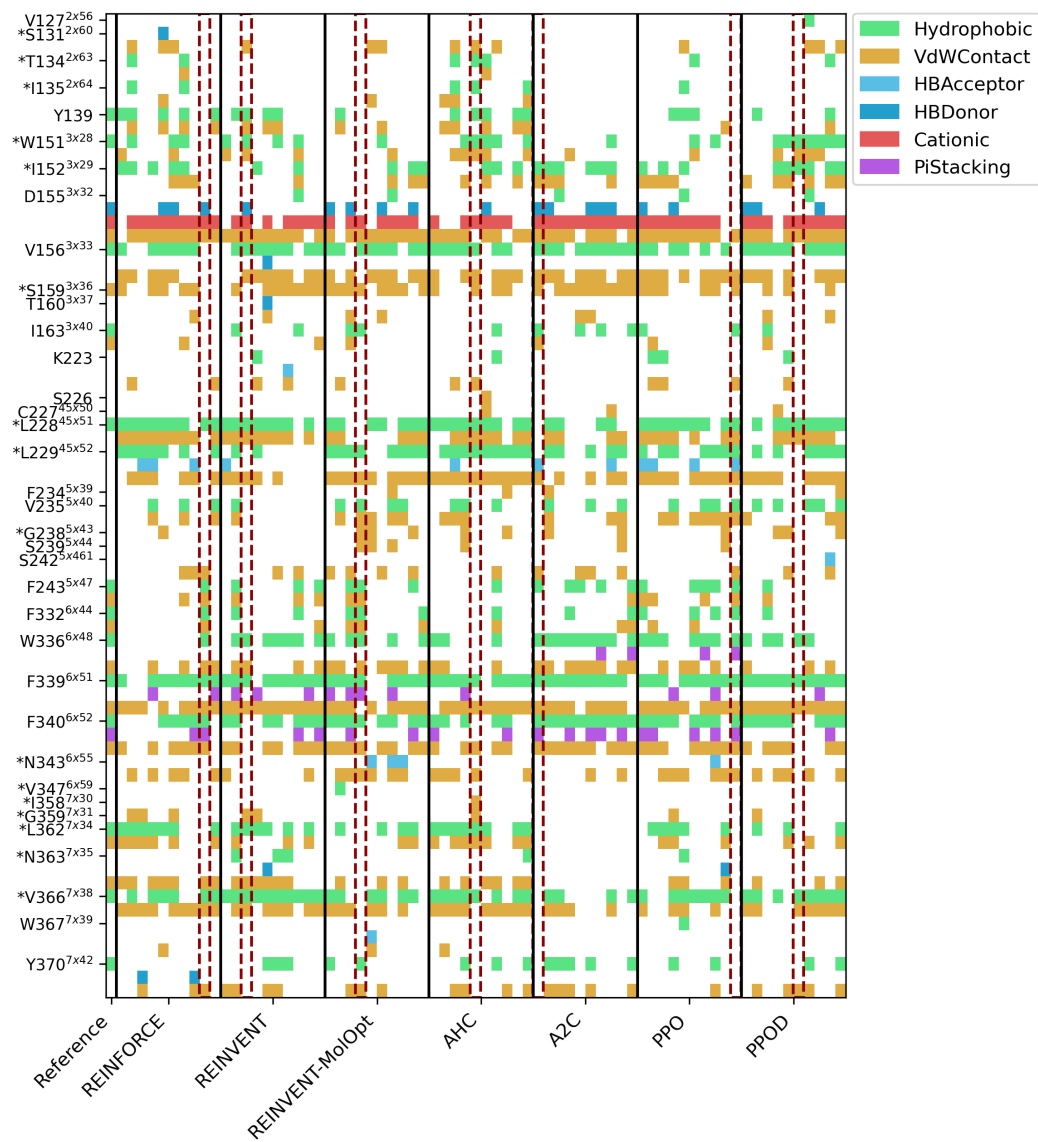


Figure 14: Protein ligand interaction fingerprints of the top 10 compounds proposed by each RL algorithm. Examples are selected for visualization of their docking poses in Figure 1. Residue labels marked with an "*" are different for the corresponding structurally aligned residue in D₂.

F SCAFFOLD CONSTRAINED MOLECULAR GENERATION CASE STUDY

The same training dataset and pre-trained prior was used as for the MolOpt benchmark. In the first experiment, we used the objectives defined by LibINVENT Fialková et al. (2021) as re-implemented in MolScore. In the second experiment, we conducted a scaffold constrained docking experiment and took the product of three scores in the range [0-1] to define the final reward (see Table 15). The structure used was 4B05 Jeppsson et al. (2012). Note that during training, the inter-molecular rDock score was used as it was otherwise observed that RL would hack score optimization by improvement of intra-molecular rDock score only (data not shown). To discourage excessive exploitation, a diversity filter was used to penalize the re-generation of molecules via an 'occurrence' filter i.e., up to 5 duplicates resulted in no penalty, 5-10 duplicates resulted in an increasing penalty by multiplication of value scaling linearly from 1 to 0, and more than 10 duplicates resulted in a reward of 0. Both objectives and their configuration files to reproduce them can be found at <https://github.com/MorganCThomas/MolScore/>.

Scoring function	Comments	Target
5-HT _{2A} docking score (inter-molecular only)	<ul style="list-style-type: none"> - Substructure restraint based on bicyclic core - Best score of any protonated/tautomerised/isomeric variant at pH 4 - Normalized based on maximum/minimum values observed at timestep 	Minimize
Maximum number of consecutive rotatable bonds		< 3
Heavy atom count		< 50

Table 15: Description of the scoring functions to define the BACE1 scaffold constrained objective.

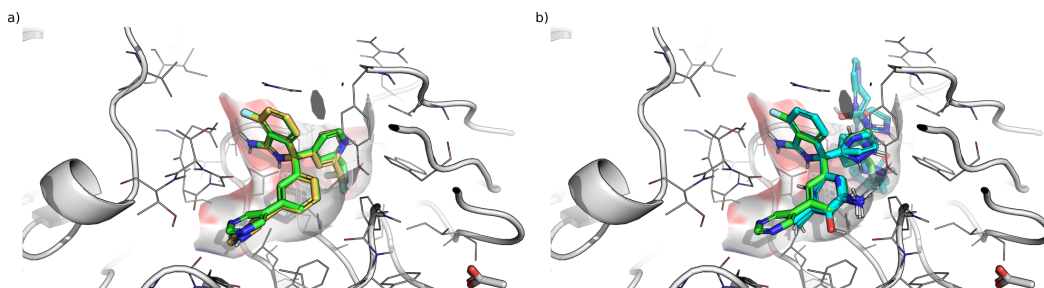


Figure 15: The docked poses of (a) AZD3839 re-docked and (b) the top 10 molecules generated by PromptSMILES with AHC. Note that the top 10 molecules often contain a secondary amine in the P1 sub-pocket to form an interaction with Tyr71 and the backbone carbonyls of Phe108 and Lys107 which interact with waters in the co-crystal structure that were removed during preparation. However, none of the top 10 molecules contain a substructure occupying the P3 sub-pocket, as the before mentioned interaction results in an orientation un-amenable to further growth into the P3 sub-pocket, although molecules outside the top 10 do show occupation of the P3 sub-pocket (data not shown).